Geophysical investigation in water rich mining area

Skenderija, Jelena

Master's thesis / Diplomski rad

2018

Degree Grantor / Ustanova koja je dodijelila akademski / stručni stupanj: **University of Zagreb, Faculty of Mining, Geology and Petroleum Engineering / Sveučilište u Zagrebu, Rudarsko-geološko-naftni fakultet**

Permanent link / Trajna poveznica: https://urn.nsk.hr/urn:nbn:hr:169:124305

Rights / Prava: In copyright / Zaštićeno autorskim pravom.

Download date / Datum preuzimanja: **2024-03-28**



Repository / Repozitorij:

Faculty of Mining, Geology and Petroleum Engineering Repository, University of Zagreb







UNIVERSITY OF ZAGREB

FACULTY OF MINING, GEOLOGY AND PETROLEUM ENGINEERING

Graduate Study of Geological Engineering

GEOPHYSICAL INVESTIGATION IN WATER RICH MINING AREA

Master's Thesis

Jelena Skenderija

GI-273

Zagreb, 2018.

Acknowledgments

This work was supported by CEEPUS network covering the study stay at Montanuniversitaet Leoben in Austria. I owe a deep sense of gratitude to Department of Applied Geosciences and Geophysics and to Univ.-Prof. Florian Bleibinhaus, for their guidance and providing necessary information regarding this research.

I would like to express my special thanks to Ao.Univ.-Prof. Robert Scholger, for imparting his knowledge and expertise in this study and for his valuable and constructive suggestions during the planning and development of this Thesis.

Also I would like to thank the management of Diabaswerk Saalfelden GmbH, Dipl.-Ing. Martin Neurauter and Dipl.-Ing. Thomas Roedhammer, and to STRABAG SE Group for the opportunity and all support for my field work and Thesis writing.

I would like to express my special gratitude to my supervisor, Assistant Professor Jasna Orešković, for her patience during reviewing the writing part of the Thesis. Her willingness to give her time so generously has been very much appreciated. My thanks and appreciations also go to Professor Franjo Šumanovac.

Finally, I would like to acknowledge with gratitude, the support and love of my parents, Gordana and Siniša, my brother David and my Alexis. I would like to thank also my friends Tihana and Mara. They all kept me going, and this Thesis would not have been possible without them.

University of Zagreb
Faculty of Mining, Geology
and Petroleum Engineering

Master's Thesis

GEOPHYSICAL INVESTIGATION IN WATER RICH MINING AREA

JELENA SKENDERIJA

Thesis completed in: **University of Zagreb**
Faculty of Mining, Geology and Petroleum Engineering
Department of Geophysical Exploration and Mining Surveying
Pierottijeva 6, 10 000 Zagreb
Montanuniversitaet Leoben
Department of Applied Geosciences and Geophysics
Chair of Applied Geophysics
Peter-Tunner-Str. 25, A - 8700 Leoben

Abstract

Geophysical research was performed in the opencast mine, the Hinterburg quarry of the Diabaswerk Saalfelden GmbH in Austria, because it already has a long history of slope problems as a result of complex structural geological conditions and difficult water conditions. According to previous research in this area, there are Paleozoic metamorphic and sediment rocks, basaltic eruptive and overlaid Quaternary alluvium moraine material. Using electrical-resistivity tomography method and seismic-refraction method, the lithological and structural relationships in the subsurface were determined as well as presence of water and its influence. Four electrical profiles (p1, p2, p3, p4) and two seismic profiles (P1 and P4) were measured. Electrical measurements were performed by multi-electrode geoelectrics using *GeoTest* software and resistivity models were obtained by *DC2DInvRes* and *Res2dinv* software. Seismic refraction measurements were performed using *Summit X One* technology and seismic velocity models were obtained by *Rayfract* software. The models obtained coincide well and they indicate a big diabase unit and metamorphic rocks together with sediment rocks and clastic moraine material. Wide range of resistivities is due to fractured rocks, caused by numerous faults, which are saturated with water that contributes the resistivity reduction.

Keywords: electrical resistivity tomography, seismic refraction, inversion, quarry, diabase rock, land sliding.

Thesis contains: 40 pages, 2 tables, 29 figures, 3 appendices and 15 references.

Original in: English

Thesis deposited in: Library of Faculty of Mining, Geology and Petroleum Engineering,
Pierottijeva 6, Zagreb

Supervisor: PhD Jasna Orešković, Assistant Professor

Technical support and assistance: Univ.-Prof. Dipl.-Geophys. Dr.rer.nat. Florian Bleibinhaus
Ao.Univ.-Prof. Dr.phil. Robert Scholger

Reviewers: PhD Jasna Orešković, Assistant Professor
PhD Franjo Šumanovac, Full Professor
PhD Snježana Mihalić Arbanas, Full Professor

Date of defense: January 19th, 2018.

Sveučilište u Zagrebu
Rudarsko-geološko-naftni fakultet

Diplomski rad

GEOFIZIČKA ISTRAŽIVANJA U RUDARSKOM PODRUČJU BOGATOM VODOM

JELENA SKENDERIJA

Diplomski rad izrađen: **Sveučilište u Zagrebu**
Rudarsko-geološko-naftni fakultet
Zavod za geofizička istraživanja i rudarska mjerenja
Pierottijeva 6, 10 000 Zagreb
Montanuniversitaet Leoben
Zavod za primijenjene geoznanosti i geofiziku
Odsjek primijenjene geofizike
Peter-Tunner-Str. 25, A - 8700 Leoben

Sažetak

Geofizička istraživanja provedena su u rudarskom području Hinterburg, u kamenolomu tvrtke Diabaswerk Saalfelden GmbH u Austriji, u kojem već duže vrijeme postoji problem klizanja terena kao posljedice složenih strukturnih geoloških uvjeta i problema s procjeđivanjem vode. Prema dosadašnjim istraživanjima, na ovom području nalaze se paleozojske metamorfne i sedimentne stijene, bazaltni eruptivi te kvartarni aluvijalni morenski materijal. Metodama električne tomografije i seizmičke refrakcije utvrđeni su litološki i strukturni odnosi, kao i prisutnost vode te njezin utjecaj. Izmjerena su četiri električna profila (p1, p2, p3, p4) te dva seizmička profila (P1 i P4). Rezultati električnih mjerenja provedeni su pomoću višeelektrodnog sustava koristeći *GeoTest* softver, a modeli otpornosti dobiveni su pomoću softvera *DC2DInvRes* i *Res2dinv*. Rezultati refrakcijskog seizmičkog mjerenja provedeni su pomoću *Summit X One* tehnologije, a modeli seizmičkih brzina dobiveni su softverom *Rayfract*. Modeli se u velikoj mjeri podudaraju i ukazuju na veliko dijabazno tijelo te metamorfne stijene zajedno sa sedimentnim stijenama i klastičnim morenskim materijalom. Širok raspon otpornosti uzrokovan je brojnim rasjedima koji stijene čine razlomljenijima te time pogodnim za infiltraciju vode koja doprinosi smanjenju otpornosti stijena.

Ključne riječi: električna tomografija, seizmička refrakcija, inverzno modeliranje, kamenolom, dijabazi, klizište.

Diplomski rad sadrži: 40 stranica, 2 tablice, 29 slika, 3 priloga i 15 referenci.

Jezik izvornika: engleski

Diplomski rad pohranjen: Knjižnica Rudarsko-geološkonaftnog fakulteta,
Pierottijeva 6, Zagreb

Voditelj: Doc. dr. sc. Jasna Orešković, RGNF

Pomoć pri izradi: Univ.-Prof. Dipl.-Geophys. Dr.rer.nat. Florian Bleibinhaus
Ao.Univ.-Prof. Dr.phil. Robert Scholger

Ocnjenjivači: Doc. dr. sc. Jasna Orešković, RGNF
Prof. dr. sc. Franjo Šumanovac, RGNF
Prof. dr. sc. Snježana Mihalić Arbanas, RGNF

Datum obrane: 19. siječnja 2018.

Table of Contents

1. Introduction 1

2. Geographical location 2

3. An overview of previous research 3

4. Geological characteristics 5

4.1. Lithological and structural characteristics of research area 5

4.2. Hydrogeology and climate 8

5. Research methods 9

5.1. Electrical-resistivity method 9

5.1.1. Electrical field measurements at the quarry location 11

5.1.1.1. *GeoTest* software 14

5.2. Seismic-refraction method 15

5.2.1. Seismic field measurements at the quarry location 16

5.2.1.1. System *Summit X One* 18

5.3. Interpretation of electrical data 19

5.4. Interpretation of seismic data 20

6. Geophysical models 23

6.1. Electrical-resistivity tomography (ERT) models 23

6.1.1. ERT model p1 24

6.1.2. ERT model p2 26

6.1.3. ERT model p3 27

6.1.4. ERT model p4 28

6.2. Seismic-refraction models 32

6.2.1. Seismic model P1 32

6.2.2. Seismic model P4 32

7. Geological interpretation 34

7.1. Geological profile GP-1 34
7.2. Geological profile GP-4 35
8. Conclusion 37
9. Bibliography 39

List of Tables

Table 1 Seismic velocities for some materials and rocks 16
Table 2 Obtained RMS errors for *Res2Dinv* and *DC2DInvRes* inversion models 19

List of Figures

Figure 2-1 Geographical location of research area (http://www.geoland.at) 2
Figure 3-1 Overview of installed 64 drainage holes, drainage system for the discharge of surface waters, 5 inclinometers (INK), 5 water observation points (P) together with *Georobot* and alerting system (Anthes et al., 2011) 4
Figure 4-1 Geological map of Austria with research area in red rectangle (customized by: http://www.arcgis.com) 6
Figure 4-2 View of the Hinterburg opencast mine from the east with the most important geological formations and two main disturbance zones (Anthes et al., 2011) 7
Figure 4-3 Detailed view of the Hinterburg opencast mine from the east with the set of faults and the main disturbance zones (Anthes et al., 2011) 7
Figure 5-1 Approximate values of resistivities for some rocks 11
Figure 5-2 Contact resistance measurement; field photo 12
Figure 5-3 Locations of the ERT profiles (*GoogleEarth* and *Surfer*) 13
Figure 5-4 Field photo showing example of installed electrode 13
Figure 5-5 Explanation of the technique to measure one geoelectric tomography profile (Rauen, 2016) 14
Figure 5-6 Locations of the seismic profiles (*GoogleEarth* and *Surfer*) 17
Figure 5-7 Hammer shooting at the beginning of the profile P1 (22nd May, 2017) 18
Figure 5-8 Field photo showing one of the remote units as part of *Summit X One* system 18
Figure 5-9 Measured and calculated apparent resistivity pseudo-sections, and the inversion model section for profile p4 in *DC2DInvRes* 20
Figure 5-10 Example of picking and reviewing first arrivals in *Rayfract* (profile P1) 22
Figure 5-11 Coverage of subsurface with the first arrival ray energy for profile P1 22
Figure 6-1 Overlapped hydraulic engineering facilities with locations of ERT profiles (*AutoCad* file; Unterberger, W., personal communication) 23
Figure 6-2 Overlapped photo (Anthes et al., 2011) with drainage holes and drainage system for the discharge of surface waters, with locations of ERT profiles 24
Figure 6-3 *DC2DInvRes* (lower) and *Res2dinv* (upper) tomography models for profile p1 25
Figure 6-4 Field photo showing cracks near the end of profile p2 26

Figure 6-5 *DC2DInvRes* (lower) and *Res2dinv* (upper) tomography models for profile p2 27
Figure 6-6 *DC2DInvRes* (lower) and *Res2dinv* (upper) tomography models for profile p3 28
Figure 6-7 *DC2DInvRes* (lower) and *Res2dinv* (upper) tomography models for profile p4 29
Figure 6-8 Rainfall [mm] with marked (blue arrow) periods of monitoring at profile p4 (https://www.salzburg.gv.at) 30
Figure 6-9 Seismic velocity model P1 32
Figure 6-10 Coverage of subsurface with first break energy for profile P4 33
Figure 6-11 Seismic velocity model P4 33
Figure 7-1 Geological profile GP-1 35
Figure 7-2 Geological profile GP-4 36

List of Appendices

Appendix 1 Spreadsheet of recording geometry for seismic model P1

Appendix 2 Spreadsheet (up) and graphic display (down) of recording geometry for seismic model P4

Appendix 3 ERT monitoring models for profile p4

List of Symbols

I - electric current [A]

V - voltage [V]

Z - impendence [V/A]

ρ - resistivity [Ωm]

L - length [m]

A - cross-sectional area [m^2]

K - constant

V_p - primary seismic wave [m/s]

V_s - secondary seismic wave [m/s]

k - bulk modulus [Pa]

μ - shear modulus [Pa]

ERT - electrical resistivity tomography

RMS - root-mean squared error [%]

Δ-t-V - triplet stands for: offset-travel time-apparent velocity

1. Introduction

The aim of this Master's Thesis is to get an insight into the subsurface of mining area by geophysical methods and correlate results with all previous information to give solutions for improving and safely continuing mining works. The research area is located in the northwestern part of Austria, in the Hinterburg quarry in Saalfelden. The opencast mine, the Hinterburg quarry of the Diabaswerk Saalfelden GmbH, already has a long history of slope problems because of complex structural geological relations and difficult water conditions. Many previous researches were done with the purpose of solving these problems, but additional geophysical research was required to gain more information.

This geophysical research as part of Master's Thesis was the first geophysical project in Diabaswerk Saalfelden. Electrical-resistivity tomography (ERT) method and seismic-refraction method have been applied to enable more detailed model of the quarry surrounding. The expected geological model contains diabase rock, metamorphic and sediment rocks and overlaid Quaternary alluvium moraine material. Electrical measurements along four profiles (p1, p2, p3, p4) were performed by multi-electrode geoelectrics using *GeoTest* software, and two seismic profiles (P1 and P4) were measured using *Summit X One* technology. Electrical profile p4 was selected for the monitoring purpose, with the aim to find out whether and how more water replenishment is influencing behavior of subsurface and does it have an influence on sliding of mining area. Electrical-resistivity tomography models and seismic models obtained by inversions are compared along two profiles where both methods were applied. Considering these models and referring to the geology of the area, obtained geological interpretation of research area is shown by two geological profiles (GP-1 and GP-4).

2. Geographical location

Saalfelden, also called Saalfelden Am Steinernen Meer, with its coordinates 47°25′37″N 12°50′54″E, is a town in the northwest Austria (Figure 2-1). It belongs to the state of Salzburg and distance between these two cities is 45 km. Elevation of Saalfelden area varies around 744 m above the sea level and micro location of research is situated 800 m above the sea level. Total urban area of Saalfelden takes 118 km^2 with approximately 16000 inhabitants. Territory of Saalfelden is basically formed by the Saalfelden Basin and is part of the Northern Limestone Alps. To the north of Basin, along German border, is Steinernes Meer high plateau. To the west of the Basin are the Leogang Mountains and the eastern part includes the Hochkönig mountain group and the Salzburg Slate Alps. Lake Zell and Salzach River are located in the generally open south part of the Basin.

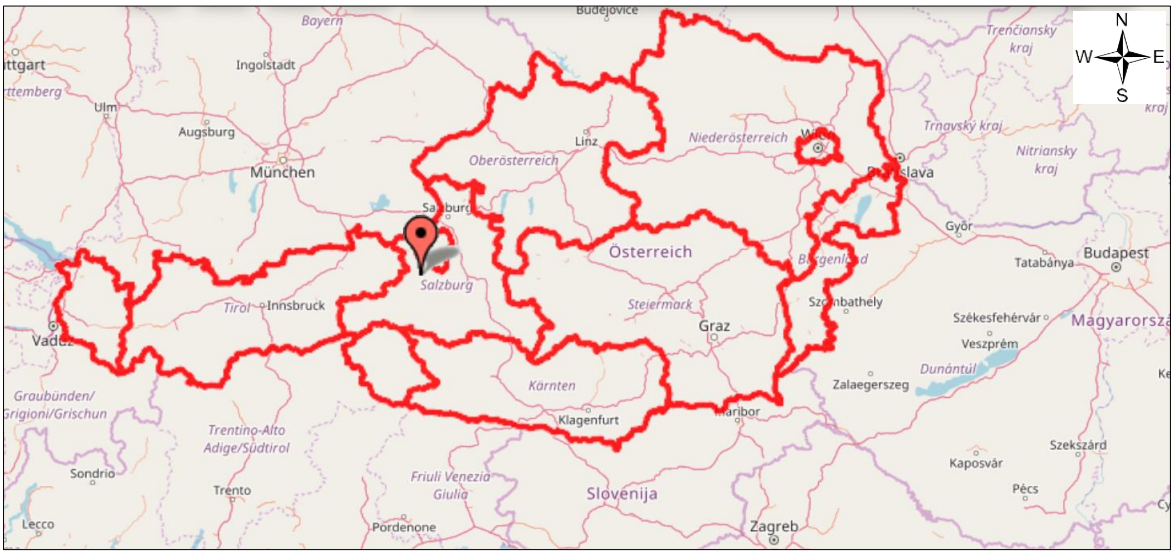


Figure 2-1 Geographical location of research area (http://www.geoland.at)

3. An overview of previous research

The Mineral Group Diabaswerk Saalfelden is part of the STRABAG South Europe (SE) Group from 2006, and one of the leading raw material brands in Central, South-East and Eastern Europe. Mining operations were phased out and replaced by the new mining facility Tagebau 21 – Schoenangerl in spring 2011.

Because of a long history of slope problems, the company was forced to deal systematically with the question of the stabilization of rock and loose rock deposits. Extensive observation programs for the early detection of slopes were set up and operated. In addition to the detection of the slope movements, the observation and control of the mountain water situation was given special attention. These slope instabilities are often closely related to abnormal mountain water situations due to the snow melting after very snowy winters or because of unusual rainfall events.

The measures to ensure the safe extraction of the diabase deposit site are described under complex geotechnical conditions, the focus being on the treatment of extreme mountain water situations. Due to the difficult geotechnical conditions and the related stability problems the company has been established more than 15 years ago a program of systematic slope monitoring and the routine recording of the geological conditions in the opencast mining area and in particular of the microstructure which changes over short distances. The geotechnical planning of the opencast mine excavations included the regular assessment of the microstructure and the geological conditions, as well as the investigation of the regional stability of the open-pit excavation. The long-term measurements are carried out by an external surveying office and the short-term measurements are carried out by the company's internal staff.

The opencast mine is intersected by two main faults, HV 1 and HV 2, which have led to a faulty decomposition of the mountains with different orientations (Figure 4-2 and Figure 4-3). These main faults were not known at the site of the quarry 40 years ago and were only approached during the excavation process (Anthes et al., 2011).

To locate the base of the mass movements in the rock, five 35 m deep bores were taken and installed in vertical inclinometers (INK). For the three-dimensional detection of the deformations at the surface, an automated geodetic measuring system called *Georobot* was

installed with a fixed robot theodolite. Also, 26 measuring points equipped with prismatic mirrors were installed in the open pit mine. The measurement points are approached by a computer-assisted control system at half-hour intervals, and the measurement data is automatically evaluated. A multi-stage alarm system is coupled to the measurements, which is activated when defined threshold values of movements are exceeded. In addition, five vertical depths of observation (P), each 50 m deep, were installed to measure the mineral water conditions (Figure 3-1). They were equipped with automatic measuring transducers, called dividers, which continually record the groundwater level or pressure levels and the groundwater temperature at the levels (Anthes et al., 2011).

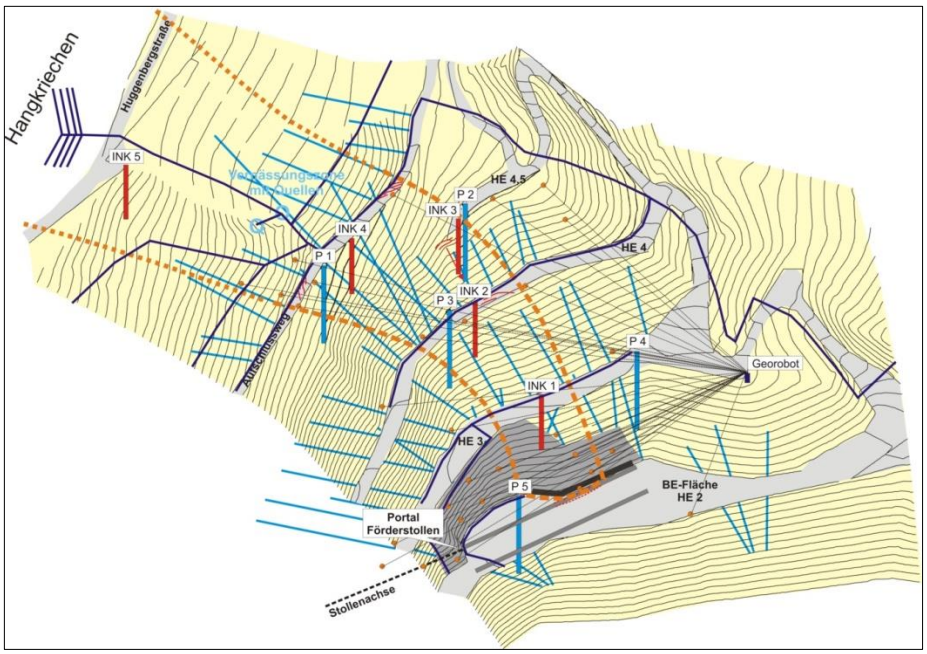


Figure 3-1 Overview of installed 64 drainage holes, drainage system for the discharge of surface waters, 5 inclinometers (INK), 5 water observation points (P) together with *Georobot* and alerting system (Anthes et al., 2011)

4. Geological characteristics

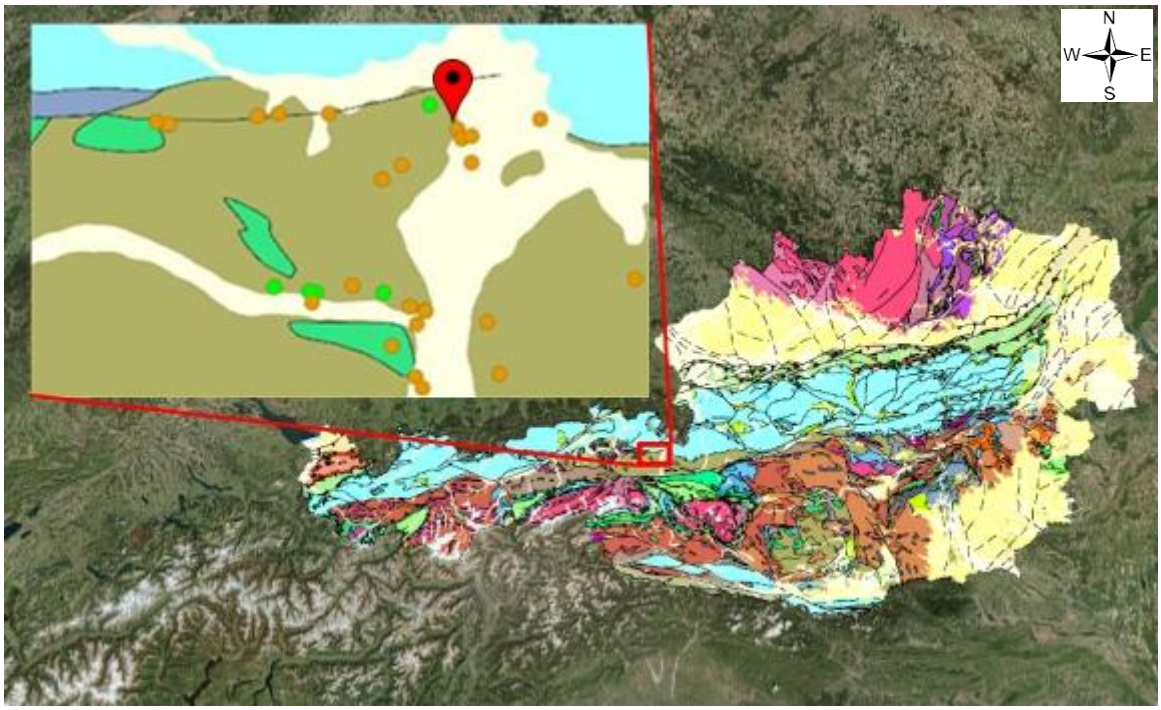
4.1. Lithological and structural characteristics of research area

Geological situation at the research area of Saalfelden is presented within geological map of the Austria, with their narrow environment for describing the general geology of this area (Figure 4-1). Research area is situated at the boundary of two specific geology domains; older Cambrian – Devon metamorphic rock presented with slate, phyllite and greywacke, together with the youngest alluvium Quaternary where Pleistocene deposits are along the main drainage lines and moraines in the Alpine foothills. Generally, this area includes alluvium moraine deposits, sedimentary rocks, significant metamorphic rocks and diabase rock that is actually the raw material for this quarry.

The Hinterburg opencast mine of the Diabaswerk Saalfelden GmbH was laid out about 40 years ago as a slope settlement at the foot of the Biberg west of Saalfelden within the geological unit of the Northern Greywacke zone (NGZ). The NGZ is an E-W-striking tectonic unit of weakly metamorphic sedimentary and volcanic rocks of Silurian-Devonian age, which descends to the north under the Northern Limestone Alps and is bounded in the south by the Salzachtal disturbance and the Tauern crystal. In opencast mining in Hinterburg, diabase rocks are mined, which is intruded in a series of meta-sediments, called Wildschoenauer schists. The quarry is characterized by an intensive lithological change of rock units, caused by genetic processes, metamorphic overgrowth and multiple tectonic genesis. As a result, there is a close interchange of heavily weathered rocks, such as clay slate and graphite-bearing phyllite as well as weather-resistant greywacke, quartzite and diabase. In the recent geological period, the entire NGZ and thus also the opencast mining area have been strongly overwhelmed by glacial processes (Anthes et al., 2011).

Figure 4-2 is giving an overview of opencast mine in Hinterburg with the most important geological information. At the Hinterburg quarry, there are complex storage conditions of diabase, greywacke and quartzite as well as clay shales and phyllite. The mountain is characterized by very high degree of decomposition with a separation surface structure that varies greatly in size. As mentioned before, the opencast mine is intersected by two main faults, HV 1 and HV 2, which have led to faulty fractured mountains with different orientations. It is important to mention that these two faults are highlighted and

their position is approximately shown. Also, it is important to notice that there are numerous smaller faults that appear in parallel sets or crossing each other, as well as main faults (Figure 4-3).



Legend of featured area:

- Slate, phyllite, greywacke; CAMBRIAN – DEVON
- Greenschist, diabase; late ORDOVICIAN – DEVON
- Marble; late ORDOVICIAN – DEVON
- Limestone, dolomite, marl, marlstone, slate, sandstone; PERM – early CRETACEOUS
- QUATERNARY (Alluvium; PLEISTOCENE along the main drainage lines and moraines in the Alpine foothills)
- Tectonic line; shear zone; Tyrolean-Noric system
- Industrial mineral; raw material – Diabase
- Mineral Pyrite; raw material – Fe

Figure 4-1 Geological map of Austria with research area in red rectangle (customized by: http://www.arcgis.com)

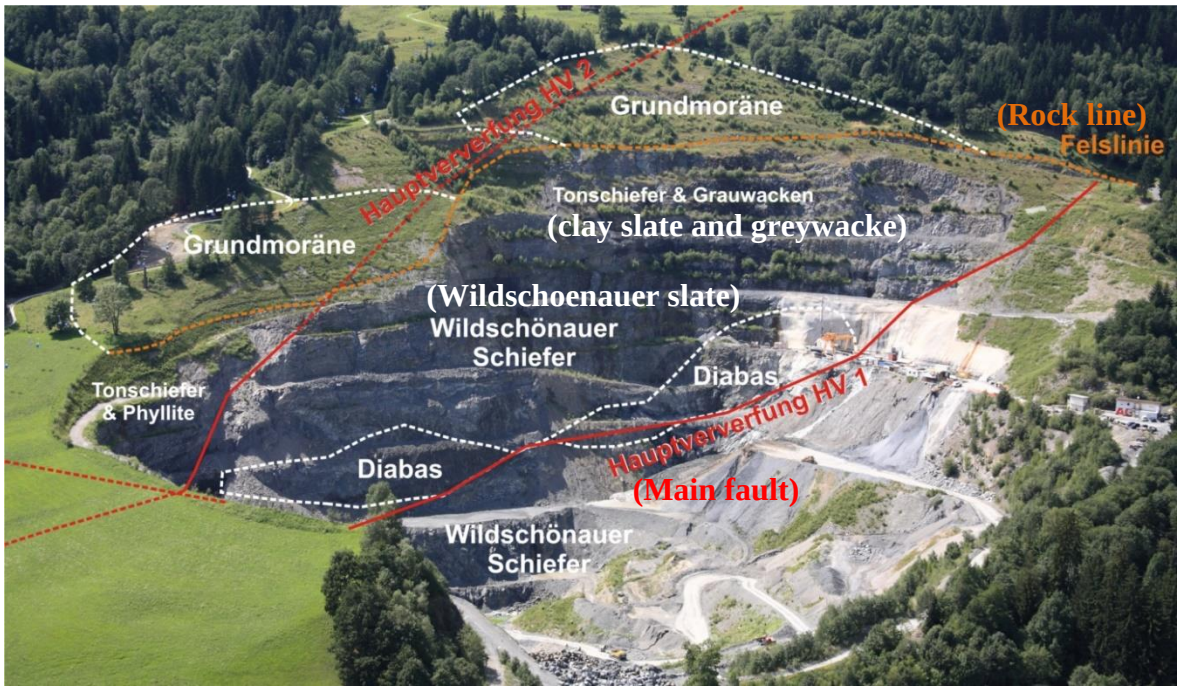


Figure 4-2 View of the Hinterburg opencast mine from the east with the most important geological formations and two main disturbance zones (Anthes et al., 2011)

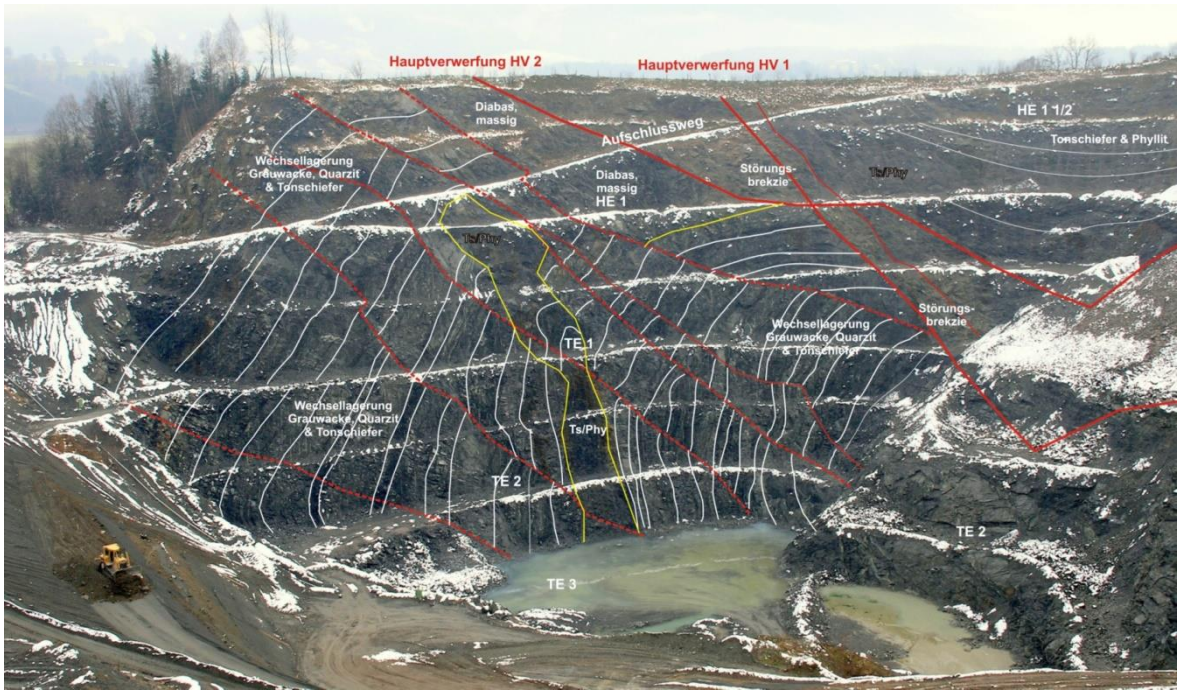


Figure 4-3 Detailed view of the Hinterburg opencast mine from the east with the set of faults and the main disturbance zones (Anthes et al., 2011)

4.2. Hydrogeology and climate

Austria is water rich country with an average rainfall of about 1100 mm per year and nearly the whole drinking water supply is based on groundwater. About one half of the population gets its drinking water from springs and the other half is supplied by groundwater in Quaternary sediments of valleys and basins (Winkler and Hilberg, 2016). As is shown in geological description of research area, there are also Quaternary sediments and the area is situated in big basin, so water supply is at high level. On the other hand, as research area is located at the boundary of two geologically different parts, different hydrogeological situation is expected there. Accordingly, where igneous and metamorphic rocks prevail, springs with generally low yield (<5 l/s) are the basis for the drinking water supply (Goldbrunner, 2000), and those are Paleozoic deposits.

Also, Saalfelden territory is a part of the Northern Limestone Alps which are well known as areas with the richest water resources. Reason for this are on the one hand rich rainfall, on the other hand the wide spreading of intensively karstified rocks. Areas whose subsurface consists of crystalline rocks or of clays and marls generally have a lower groundwater level.

How water regulates the climate, research area is characterized by high precipitation where prevail continental influenced conditions with colder winters and rather warm summers. The diversity of topographical and climatic conditions results in a very versatile flora and fauna. The geographic features in the more mountainous regions of the country have given rise to yet another climate zone, the Alpine climate that causes winters to be colder than at lower altitudes. Temperatures depend largely on the altitude.

During the months June, July, August and September there are nice average temperatures. Most rainfall is seen in May, June, July and August. On average, the warmest month is August with an average maximum temperature 23 °C and the coolest month is January with an average minimum temperature of -5 °C. July is the wettest month with an average precipitation 170 mm and February is the driest month with an average precipitation of 65 mm (https://weather-and-climate.com).

5. Research methods

For the purpose of geophysical investigation of mass movement in mining area of Saalfelden, two methods were used: electrical-resistivity method and seismic-refraction method. Both were used with the aim to get more subsurface information using different methods and trying to reduce ambiguity by their correlation and final interpretation. During interpretation, electrical and seismic results were also correlated with existing water hydraulic engineering facilities, especially drainage positions and also including all field notes made in field work and measurements. Considering electrical resistivities, seismic velocities, as well as drainage positions and water situation, the geology of the research area was interpreted.

5.1. Electrical-resistivity method

Geoelectric methods are based on measurements of electrical properties of rocks. Based on the measured resistivities it is possible to gain knowledge about lithology of the deposits and their condition, as compactness, porosity, fissures, but also to gain knowledge about water quality, e.g. salinity and mineralization.

Resistivity methods are based on injection of electric current *I* [amperes, A] into the ground through the pair of the electrodes and afterward resulting voltage *V* [volts, V] is measured between a second pair of electrodes. Further ratio of the voltage output *V* measured at the potential electrodes to the current input *I* at the current electrodes, presents an electrical impendence Z of the subsurface (Everett, 2013):

$$Z = \frac{V}{I} \left[\frac{\mathrm{V}}{\mathrm{A}}\right] \tag{5.1}$$

The voltage *V* is defined by the expression:

$$V = \rho I \frac{L}{A} \ [\mathrm{V}] \tag{5.2}$$

Consider a cylindrical sample of material, ρ presents resistivity [ohm-meters, Ωm], *I* is electric current [amperes, A], *L* is length [meters, m] and *A* is a cross-sectional area [square meter, m^2]. Due to their direct connection, the form for calculating the resistivity is derived from the voltage expression:

$$\rho = K\frac{\Delta V}{I}\ [\Omega\mathrm{m}], \tag{5.3}$$

where K is constant which depends on geometrical arrangement of electrodes and ΔV is voltage difference.

If underground is electrically homogeneous, measuring results are the real material resistivities, otherwise results are an apparent resistivities that depends on the resistivities of the individual rocks. The flow of electric current depends on the spacing of the electrodes, so the larger distance means a deeper penetration, while a smaller distance is used for the shallower coverage.

A map of the apparent resistivity plotted at these locations is termed a pseudo-section (Loke, 2000). The pseudo-section is then inverted to obtain a two- or three-dimensional (2-D or 3-D) resistivity section of the ground, known as electrical resistivity tomography (ERT). Because of the assumption about 2-D resistivity section of the ground, that means resistivities can change longitudinally and vertically, the main advantage of method is possibility of mapping the area with complex geological conditions (Griffiths and Barker, 1993).

Finally, a geological interpretation of the resistivity section is performed and relevance of the model depends on the differences in the resistivities, i.e. for the larger resistivity contrast the more precise interpretation results can be expected.

The rocks differ in resistivity, but the same rock may have resistivity in very wide ranges so there are overlapping in resistivities of different rocks in wide proportions (Figure 5-1).

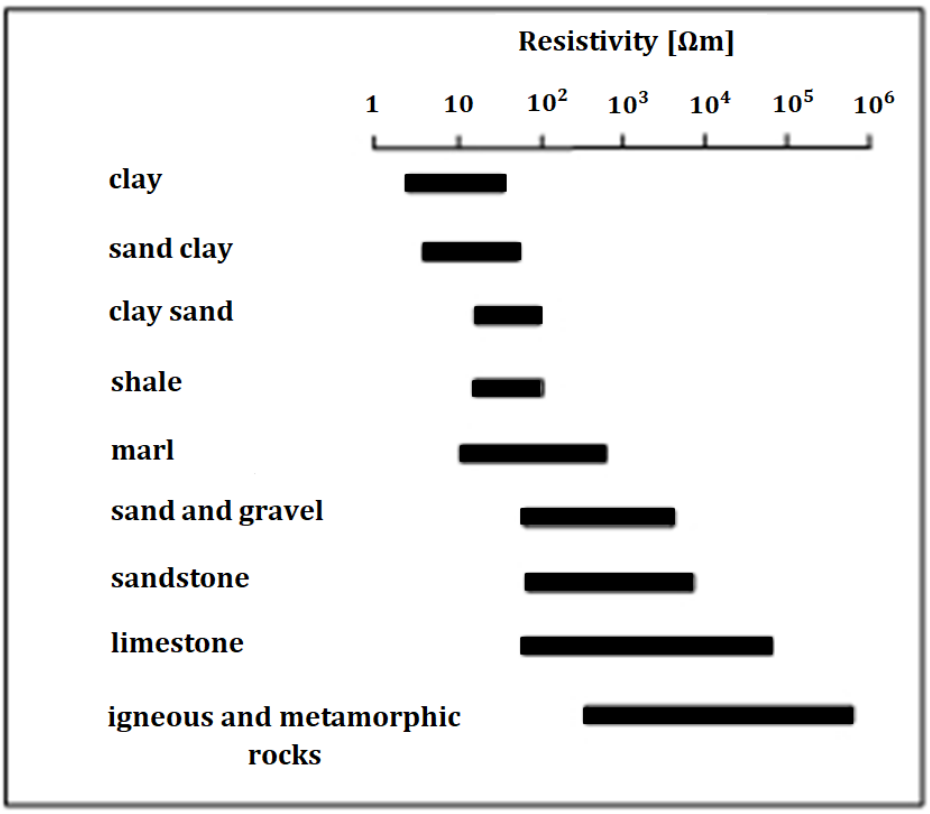


Figure 5-1 Approximate values of resistivities for some rocks

5.1.1. Electrical field measurements at the quarry location

Most of the quarry area was covered with geophysical investigation measurements. Therefore, four profiles have been set as shown in Figure 5-3. Length of profile p1, profile p2 and profile p3 is 495 m and profile p4 is 250 m long.

After placing profile using measuring tape and trying to make it straight as possible, metal sticks were placed every 5 m into the ground using hammer and then electrodes were connected to them. At the beginning of profile, equipment for collecting data was set up. One more ground electrode was placed near to the equipment and connected with it via cable. Before starting measurements, people were warned about safety requirements because geoelectric devices can produce high electrical voltages of 200 volts or more.

After setting up all parameters, both in measuring device and computer, measurements were performed. If some electrodes were showing extremely different results during the contact resistance measurement they were fixed and measurements were repeated (Figure 5-2).

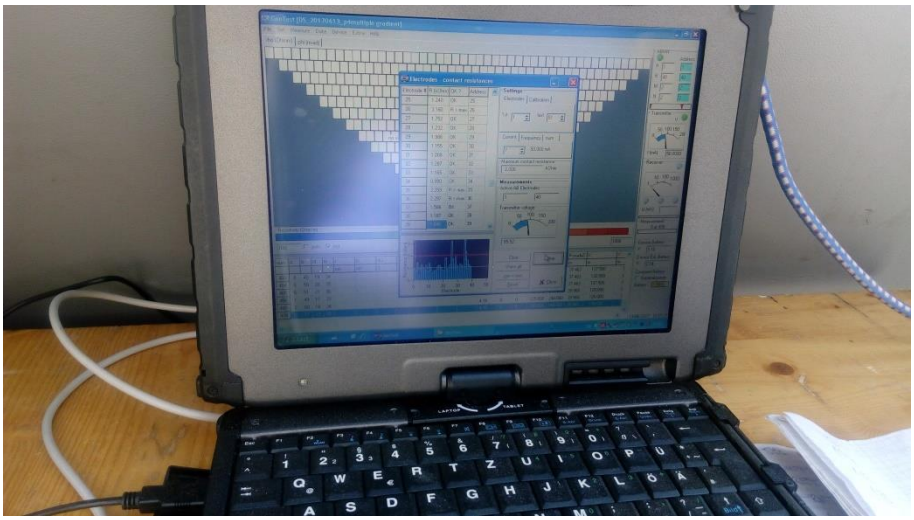


Figure 5-2 Contact resistance measurement; field photo

The measurements were performed by Wenner electrode configuration with 5 m electrode spacing by multi-electrode geoelectrics using *GeoTest* software. Coordinates of electrode positions were collected by *Trimble 4700* GPS system and afterward digitized using *Surfer* software. The equipment is produced by the German *LGM - Erich Lippmann Company*. Altogether 100 electrodes were used on profiles p1, p2, and p3 and on smaller profile p4 were used 51 electrodes. One of the electrodes is shown in Figure 5-4.

ERT field measurements were performed 4 times, in April, May and twice in June 2017. After the 1st field surveying, profile p4 was chosen as one for the monitoring purpose. Other three ERT field measurement were done only with the aim of monitoring profile p4. Monitoring was done before and after big rain event. Idea was to try to find out whether and how more water replenishment is influencing behavior of subsurface and does it have an influence on sliding of mining area. Also, it was shown how existing drainage pipes and whole drainage systems are working and help in the water drainage.

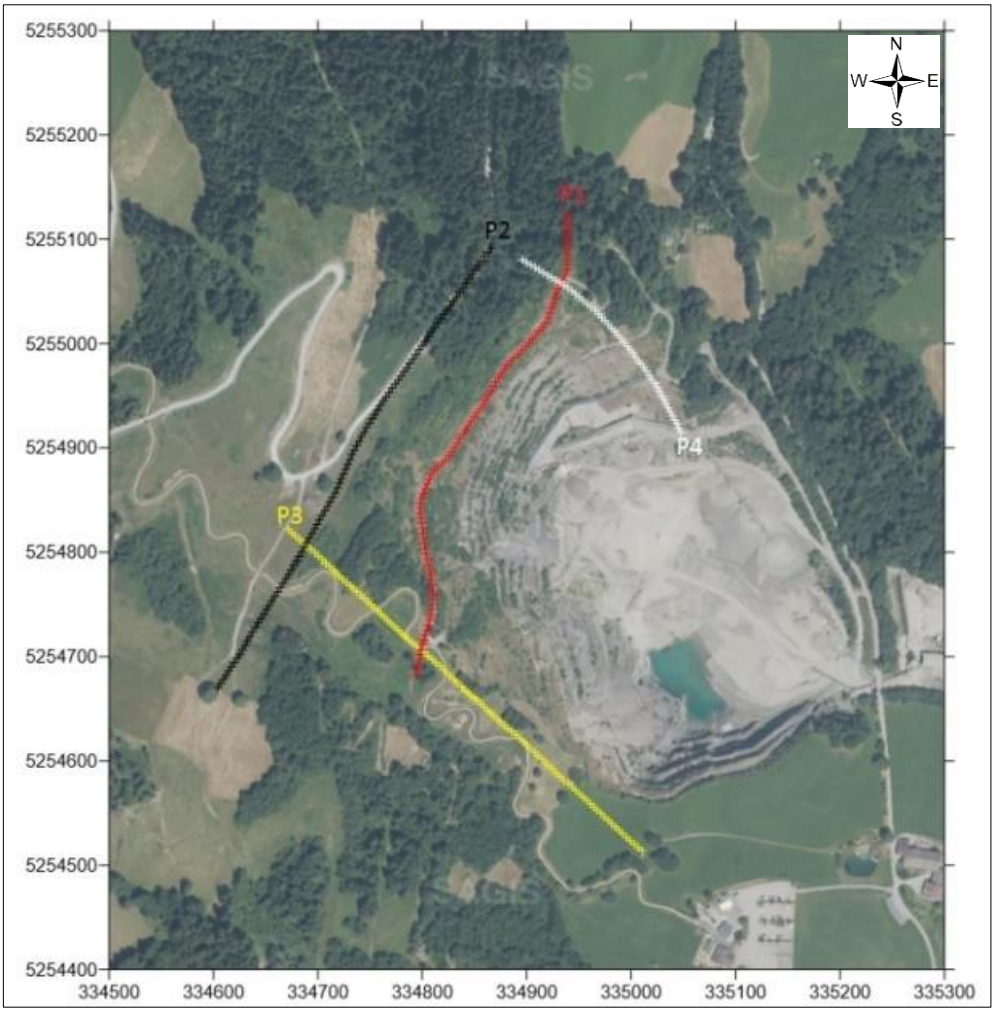


Figure 5-3 Locations of the ERT profiles (*GoogleEarth* and *Surfer*)



Figure 5-4 Field photo showing example of installed electrode

5.1.1.1. *GeoTest* software

This software is used for controlling geoelectric equipment in combination with many electrodes, called "Multielectrode Geoelectrics". Using two-dimensional or three-dimensional inversion techniques additionally for evaluation, this 4-point geoelectrics method is known for Geoelectric tomography or Electrical resistivity tomography (Figure 5-5). Two electrodes serve as current emitting electrodes and these are usually named A and B. Two other electrodes measure the potential difference (voltage) and these are the M and N electrodes (Rauen, 2016).

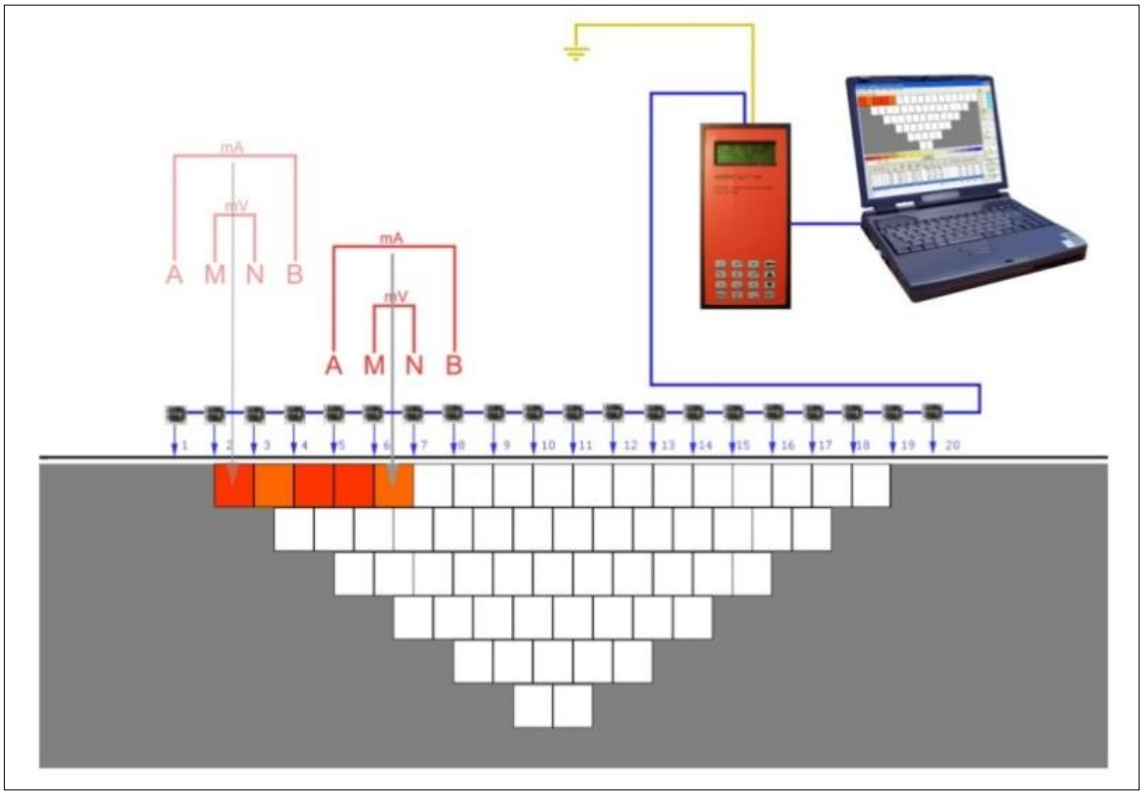


Figure 5-5 Explanation of the technique to measure one geoelectric tomography profile (Rauen, 2016)

5.2. Seismic-refraction method

The seismic-refraction method is based on the refraction of seismic energy at the interfaces of geological layers of different velocities. Seismic refraction can identify variations in material type with depth and their lateral position. The technique images the interfaces between materials with contrasting seismic velocities. This translates to differences in the elastic properties and/or density of the material.

Velocities of primary V_p and secondary V_s seismic waves depend on density and elastic moduli:

$$V_p = \sqrt{\frac{k+\frac{4\mu}{3}}{\rho}}\left[\frac{\mathrm{m}}{\mathrm{s}}\right], \tag{5.4}$$

where *k* represents bulk modulus, μ is shear modulus and ρ is resistivity.

$$V_s = \sqrt{\frac{\mu}{\rho}}\,[\mathrm{m/s}] \tag{5.5}$$

From their ratio is obvious that primary waves are faster, $V_p > V_s$.

Each wave on the boundary of areas with different velocities is partially reflected and partially refracted. Therefore, Snell's law can be applied:

$$\frac{sin\theta_1}{V_1} = \frac{sin\theta_2}{V_2} \tag{5.6}$$

Seismic velocities are greater with the greater density of the rocks because of grain structure of the rock materials (Šumanovac, 2007). How elastic modulus of rocks are decreasing with compactness, and they are also decreasing faster than bulk density, it is a reason of faster decreasing of seismic velocities with decreasing densities.

Table 1 shows wide range of seismic velocities of different materials that is explained by their widely different saturation, consolidation, weathering, fractioning and homogeneity.

Table 1 Seismic velocities for some materials and rocks

Material	Vp (m/s)
AIR	330
SOIL	100 - 600
SAND (dry)	300 - 900
SAND (saturated)	1000 - 2000
CLAY	900 - 2500
WATER	1450
SANDSTONE	1500 - 4000
SANDSTONE (por. and sat.)	2000 - 4500
GLACIAL MORAINE	1500 - 2700
WEATHERED igneous and metamorphic rock	450 - 3700
WEATHERED sedimentary rock	600 - 3000
SHALE	800 -3700
METAMORPHIC ROCK	2400 - 6000
UNWEATHERED BASALT	2600 - 5000

5.2.1. Seismic field measurements at the quarry location

As mentioned before, in order to get more information about subsurface, seismic-refraction method was performed to get more data using different parameters. Seismic measurements were performed on 3rd field work, 22nd and 24th May, 2017.

Two seismic profiles, P1 and P4, were measured that were trying to be along ERT profiles p1 and p4 as is shown in Figure 5-6. Length of the profile P1 is 476 m and contains 120 geophones, and length of the profile P4 is 180 m with 46 geophones.

After setting profiles using measuring tape and trying to make it straight as possible, geophones have been placed every 4 m. Cables were set up along the entire profile and afterward remote units were snapped on. All shot data were collected into the computer that has been set up at the beginning of profiles.

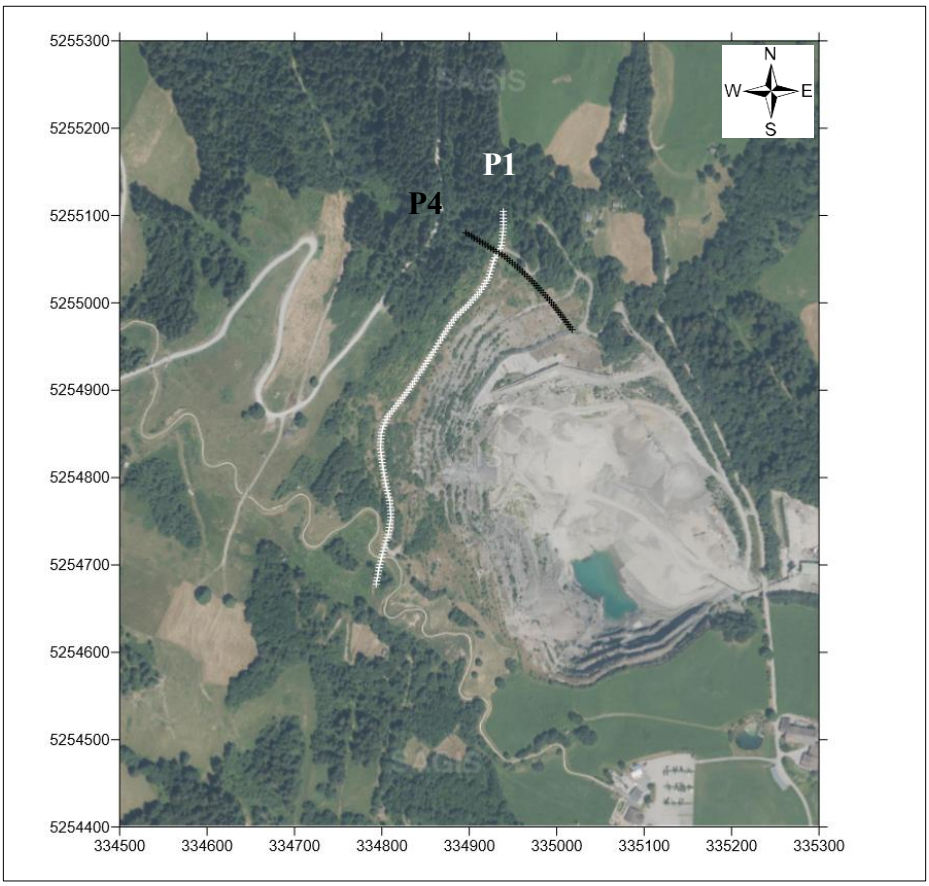


Figure 5-6 Locations of the seismic profiles (*GoogleEarth* and *Surfer*)

At the profile P1 hammer shots every 8 m were performed. So, there were totally 61 hammer shots (Figure 5-7) and also 6 explosive shots, three at the beginning (0 m, 24 m, 48 m) and three at the end of the profile (428 m, 460 m, 476 m). At the profile P4 only 3 hammer shots P4 were done, on positions 44 m, 136 m and 180 m. The measurements were performed by *Summit X One* technology from the German *DMT Company*. Geophone spacing was 4 m and their coordinates were collected by *Trimble 4700* GPS system and afterward digitized using *Surfer* software. Spreadsheet of recording geometry for seismic model P1 is shown in Appendix 1 and it includes recording numbers, geophone positions,

altitudes, northing, easting and positions along the profile. Appendix 2 shows spreadsheet and graphic display of recording geometry for seismic model P4.



Figure 5-7 Hammer shooting at the beginning of the profile P1 (22nd May, 2017)

5.2.1.1. System *Summit X One*

Summit X One represents flexible cable bound seismic data acquisition system. With ultra-small remote units (Figure 5-8) connected to a lightweight telemetry cable at any position, all station distances can be realized with the same cable. From the *Summit X One* brochure by *DMT GmbH & Co. KG Company*, this SUMMIT 'Snap-on' technology provides great solution for high resolution 2-D and 3-D seismic measurements in any terrain with flexible station distances in the range from one to several meters. It has also an option for continuously recording which is suitable for passive seismic applications.



Figure 5-8 Field photo showing one of the remote units as part of *Summit X One* system

5.3. Interpretation of electrical data

Electrical resistivity data were collected using *GeoTest* software. With the obtained data inversions were performed using *DC2DInvRes* and *Res2dinv* software. Before starting inversions, data were prepared in .txt form, including recorded altitudes, positions along the profile, northing and easting. In *DC2DInvRes* it was attempted to get the best results by manually changing some parameters, while *Res2DInv* has automatically determining a two-dimensional (2-D) resistivity model for the subsurface based on data obtained from electrical imaging surveys (Griffiths and Barker 1993). Both inversions together gave satisfying results which are shown in Chapter 6.

Considering inversion results from both programs, there is a question which program, i.e. what results we should “trust” more. Answer is that there is no correct answer. The optimization method basically tries to reduce the difference between the calculated and measured apparent resistivity values by adjusting the resistivity of the model blocks (Figure 5-9). A measure of this difference is given by the root-mean squared (RMS) error. The obtained RMS errors for both programs are given in Table 2, where we can see that the results of *DC2DInvRes* program are with noticeably greater RMS error. However, the model with the lowest possible RMS error can sometimes show large and unrealistic variations in the model resistivity values and might not always be the "best" model from a geological perspective.

Table 2 Obtained RMS errors for *Res2Dinv* and *DC2DInvRes* inversion models

	RMS error [%]	
	Res2DInv	DC2DInvRes
p1	5,3	12,1
p2	5,0	23,8
p3	16,4	8,0
p4	7,1	9,3

It can be seen that *DC2DInvRes* models are with the less detail and they are smoother, while *Res2DInv* models are more detailed. For the best understanding of the results, both inversion models must be considered with the great caution.

Final inversions were proceed using *Surfer* software, *AutoCAD* and put together with field notes and drainage system positions. It is important to accent that field notes are more trustable and overlapped on two inversion models, they showed very good fit with the *Res2DInv* results. This fact as well as the smaller RMS error was the reasons to rely more on the *Res2DInv* model inversion results.

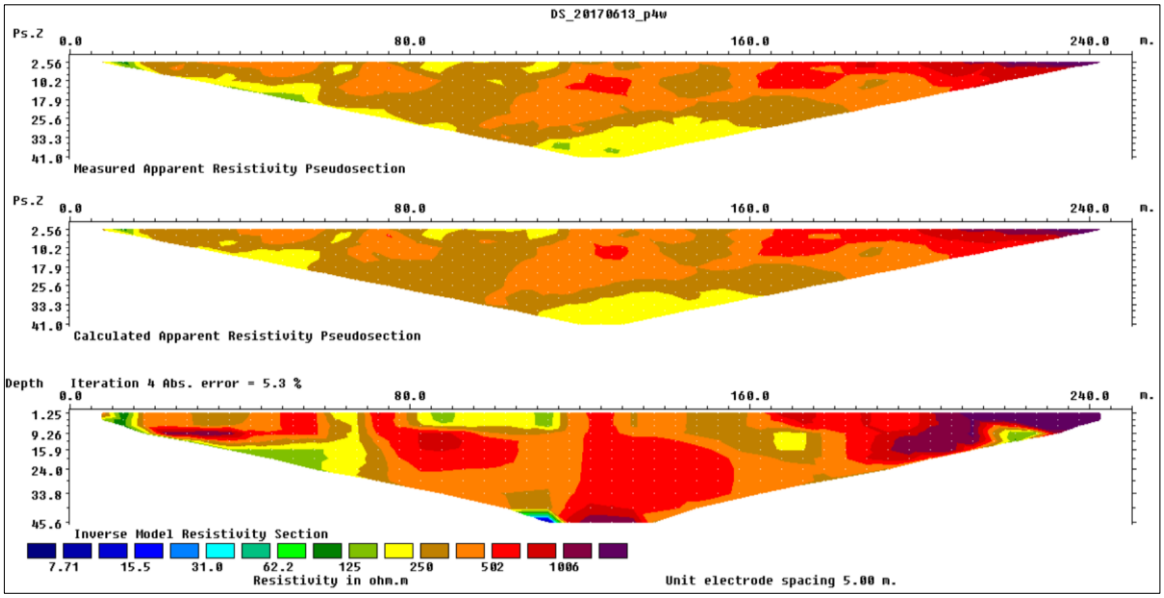


Figure 5-9 Measured and calculated apparent resistivity pseudo-sections, and the inversion model section for profile p4 in *DC2DInvRes*

5.4. Interpretation of seismic data

Recorded seismic data were interpreted during the cabinet work using the *Rayfract* software. It included picking and inverting the first arrivals for velocity structure (Figure 5-10). Then interpretation of velocity models regarding the geological features followed, with conclusion if they are consistent, or not, with resistivity models. Figure 5-11 shows model of subsurface coverage of first break energy for profile P4.

Rayfract (2006) is a software package suitable for processing of seismic profiles with low, medium or high coverage. It supports the interpretation of both P−wave and S−wave seismic refraction and borehole surveys. The process consisted of importing .sgy−data regarding to prepared recorded geometry, stacking and filtering of data, importing prepared .txt files of coordinates, picking and reviewing first arrivals, choosing inversion parameters and inversion itself.

Inversion model were obtained using *⊿-t-V* method (Gebrande and Miller, 1985). The triplet in the name of the method means that *⊿* stands for offset, *t* stands for travel time and *V* stands for apparent velocity. This method provides continuous depth-change velocity data for all positions on the refraction profile, and the interpolation of the velocity isolines yields two-dimensional section of the seismic velocities in the underground (Šumanovac, 2012). Systematic velocity increase (at the top of the basement) and strong velocity anomalies such as low velocity zones, faults etc. will be visible in many situations. From the Manual of *Rayfract* software, pseudo-2D *⊿-t-V* method generates systematic imaging artefacts in case of strong lateral velocity variation in the near-surface overburden. To eliminate these artefacts in the 1D initial model and to obtain more reliable absolute velocity estimates it was used *Smooth inversion method*.

Unlike many refraction analysis methods, *⊿-t-V* does not require the interactive assignment of travel times to hypothetical and mathematically idealized refractors. Sorting travel times by common midpoint (CMP) instead of common shot averages out the effects of dipping layers on travel times. The travel time field is smoothed naturally by stacking CMP-sorted travel time curves over a few adjacent CMP's. Then each CMP curve is independently inverted with the 1D *⊿-t-V* method (Gebrande and Miller, 1985).

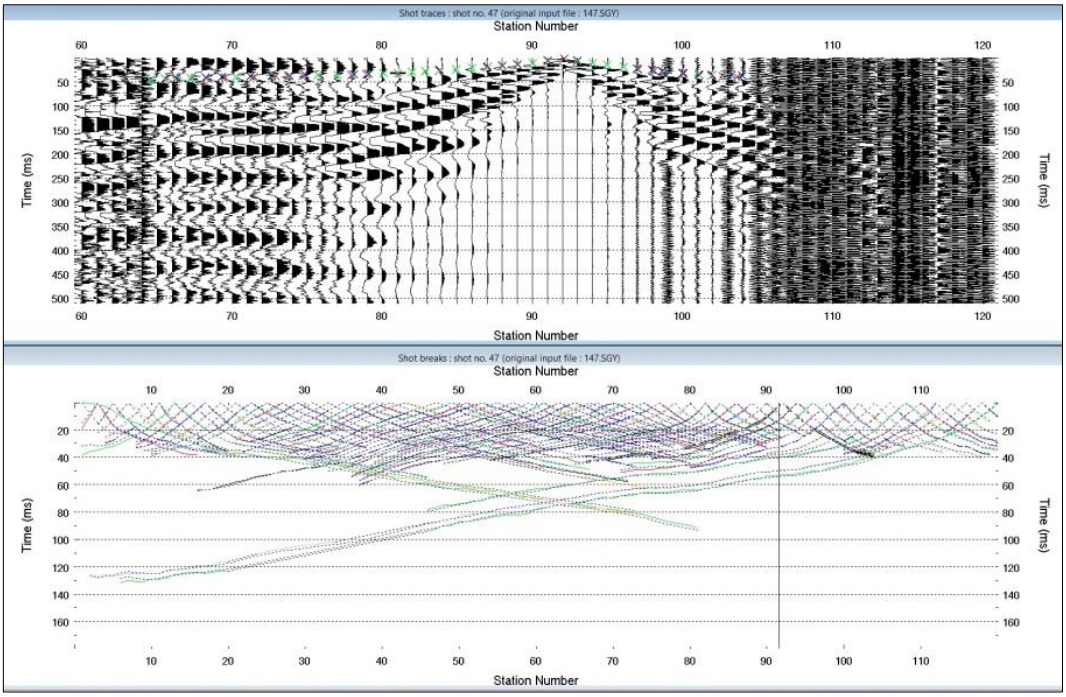


Figure 5-10 Example of picking and reviewing first arrivals in *Rayfract* (profile P1)

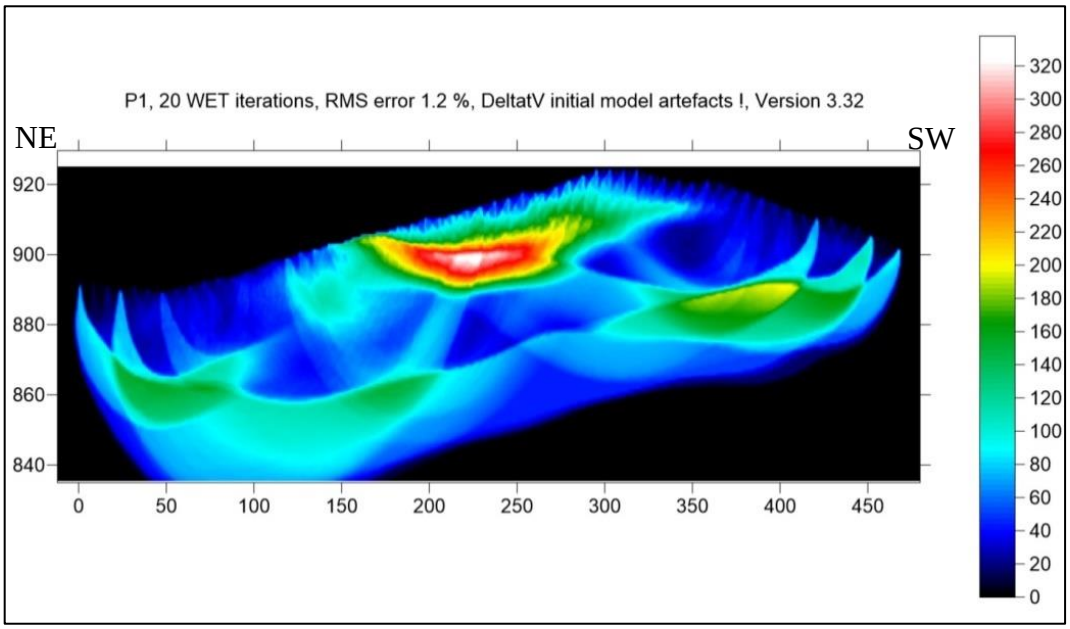


Figure 5-11 Coverage of subsurface with the first arrival ray energy for profile P1

Obtained models were processed in *Surfer* software, *AutoCAD* and correlated with ERT results together with all other important information.

6. Geophysical models

6.1. Electrical-resistivity tomography (ERT) models

Different rocks are characterized by different resistivities, but also the same rock can have resistivities in a wide range depending on a several factors. Main reasons for a wide range of resistivities are rock conditions, in term of compactness or degree of rock fracture and associated with it saturation with water.

In the following explanation of the results this fact was considered as well as previous established geological situation, present water conservation objects, especially drainage supplies, and from an engineering aspect it was given an idea and opinion of subsurface situation. Figure 6-1 shows overlapped profile locations at quarry together with *AutoCAD* file that consist information about hydraulic engineering facilities. Figure 6-2 shows overlapped profile positions at quarry with drainage pipes positions. These two figures as well as geology situation shown in Figure 4-1, helped in understanding obtained resistivities.

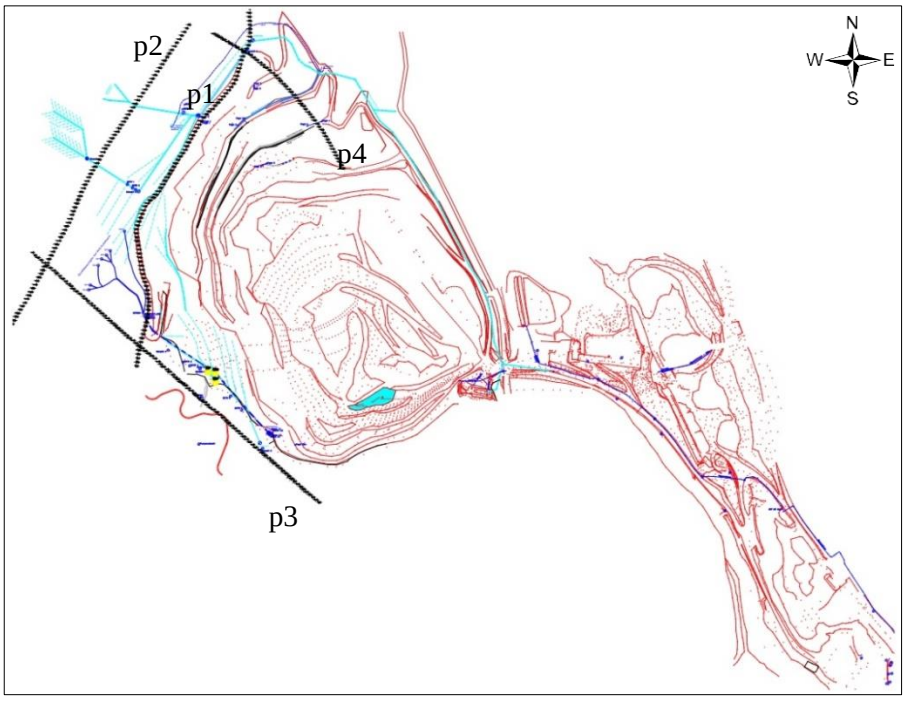


Figure 6-1 Overlapped hydraulic engineering facilities with locations of ERT profiles (*AutoCad* file; Unterberger, W., personal communication)

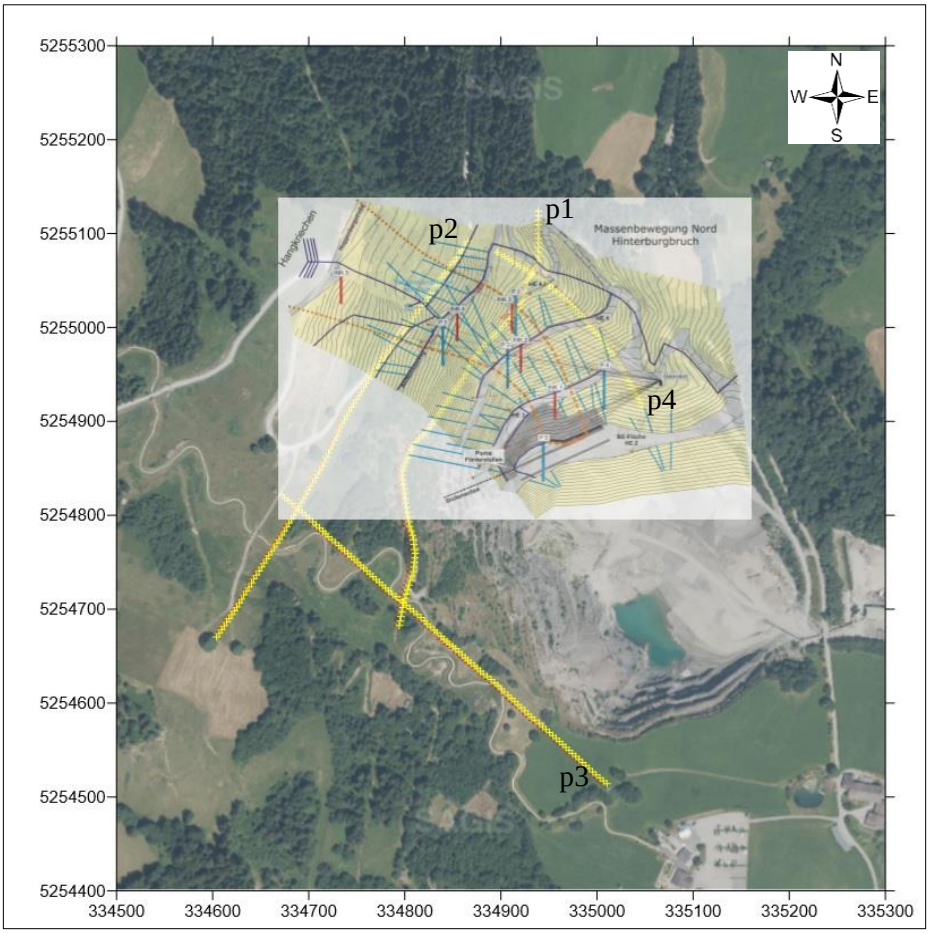


Figure 6-2 Overlapped photo (Anthes et al., 2011) with drainage holes and drainage system for the discharge of surface waters, with locations of ERT profiles

6.1.1. ERT model p1

According to Figures 6-1 and 6-2 it is shown that near profile p1 there is a water channel. Around 150 m and 430 m there are water conservation objects. Those features presented in Figure 6-3 are showing results for both *DC2DInvRes* and *Res2dinv* software. Besides, an observation can be made that there are drainage pipes from 135 m to 305 m. From this point, drainages work well.

From the field work diary, there is a big drainage system at 168 m, and at 430 m there are two big drainage systems which are filling with water. At the first part of profile, at 69 m, there is manhole. It's also important to mention that through all these profile there are drainage pipes more or less in function. Generally, drainages at 168 m and 430 m are efficient. Even broken one, drainage at 285 m is still working well. To increase efficiently it needs to be repaired.

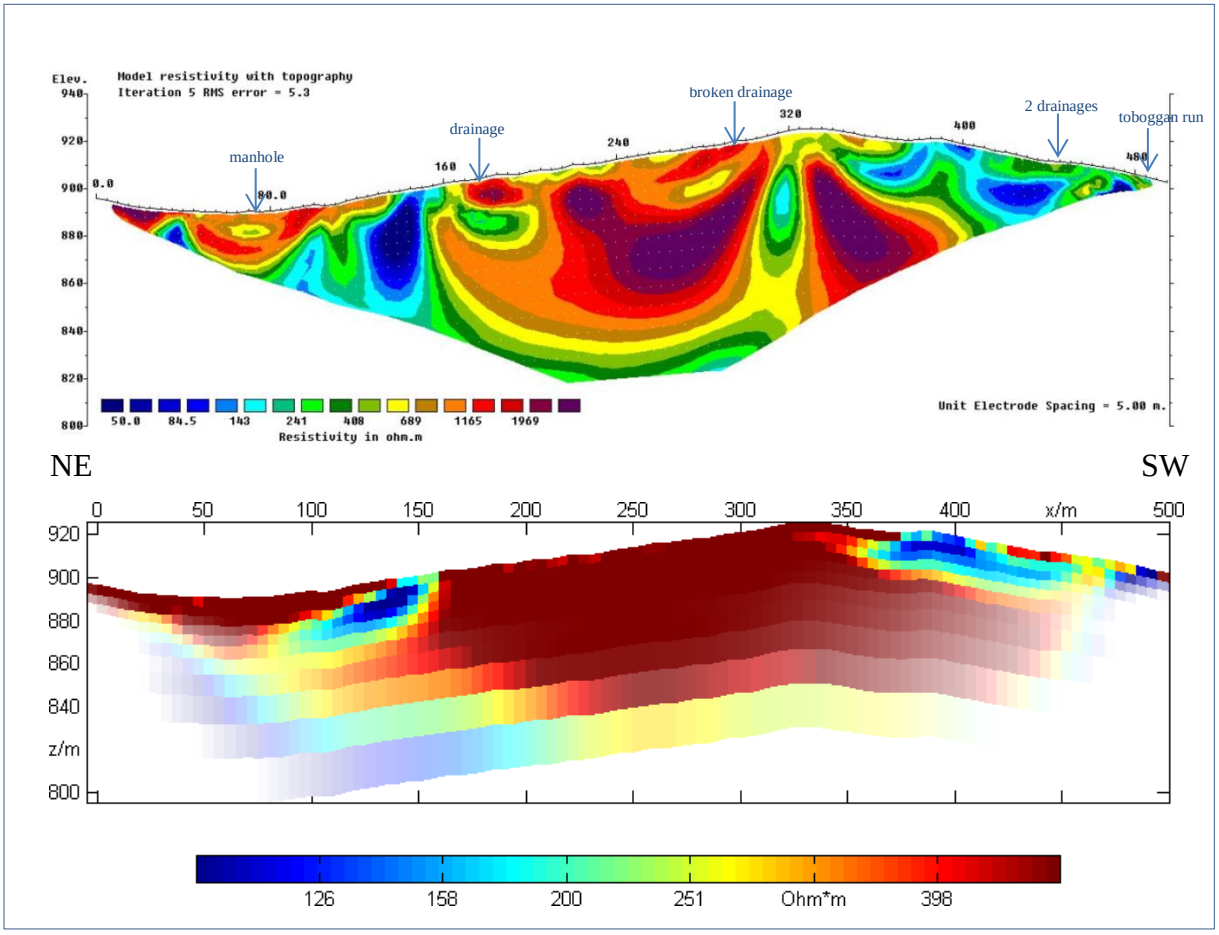


Figure 6-3 *DC2DInvRes* (lower) and *Res2dinv* (upper) tomography models for profile p1

High resistivity body with striking parts of much lower resistivities can be notices in the central part of the profile. From lithological point of view, as will be shown with geological profiles, lower resistivities are caused by two faults noticed in earlier studies of the quarry. High resistivity body is fractured and then saturated with water. Therefore, it will be important to consider these two faults in the sense of their striking, and try to protect particularly these areas, since the greatest amount of potential water presence is considered with these two faults.

Two models are generally fitting. The most visible is high resistivity from approximately 160 m – 320 m. That area includes drainage system for the discharge of surface waters that obviously work very well. From the other side, at the end of profile there is no any drainage system, 360 m – 490 m, where lower resistivity area is present.

Very significant shape of strikingly lower resistivity than its surrounding around 150 m is interpreted as fault.

6.1.2. ERT model p2

Electrical profile p2 is situated about 100 m above profile p1 and is parallel with it. At the end of profile there are a lot visible cracks (Figure 6-4). Also, in earlier studies, it was revealed that this area is moving 2 cm per year (Anthes et al., 2011).



Figure 6-4 Field photo showing cracks near the end of profile p2

According to Figures 6-1 and 6-2 there is a sub horizontal drainage system from 15 m to 175 m that also supports higher resistivities in obtained models (Figure 6-5), so this system is working really good. If profile p2 is set in relation with profile p1, it can be seen that the water saturated lower resistivity areas are matching, but the profile 2 is above and because of that better drained. Two very low resistivity areas, at 150 m and 330 m, are caused by faults.

Very significant is relatively large difference in inversion models obtained by two softwares. If we consider that profiles p1 and p2 are supposed to be rather similar, as *Res2dinv* model confirms, there is obviously something wrong with *DC2DInvRes* model for profile p2. Table 2 also shows the greatest RMS error for this model and such irregularity can be explained with insufficiently defined parameters during inversion.

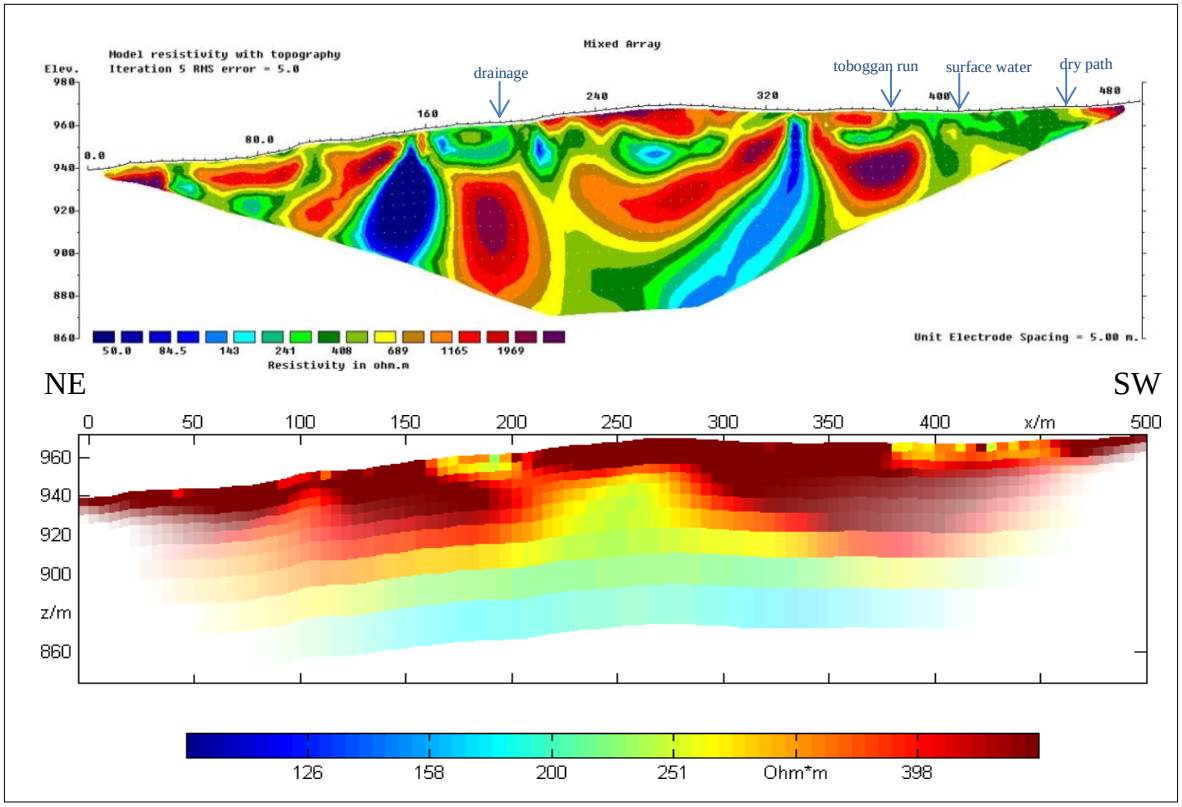


Figure 6-5 *DC2DInvRes* (lower) and *Res2dinv* (upper) tomography models for profile p2

6.1.3. ERT model p3

ERT profile p3 is orthogonal to profiles p1 and p2 (Figure 5-3). Profile p3 generally follows summer toboggan run, a touristic attraction of this area, and in several points crossing it. Results of inversion for profile p3 are presented with Figure 6-6. Noticeable blue araes with low resistivity are associated with moraines. Also, betwen 275 m and 295 m there are drill holes that also confirmed the moraine. At 295 m there is a pump and at 380 m – 395 m are two manholes. Parallel to profile 3 there are water conservation objects, from 80 m to 380 m.

The field notes show that there is a drainage pump at 394 m and at 495 m ending drainage pipe. From obtained resistivity model it could be said that drainages here are not working so well. This area must be much more drained and protected from sliding, especially because it includes summer toboggan run which requires high security level.

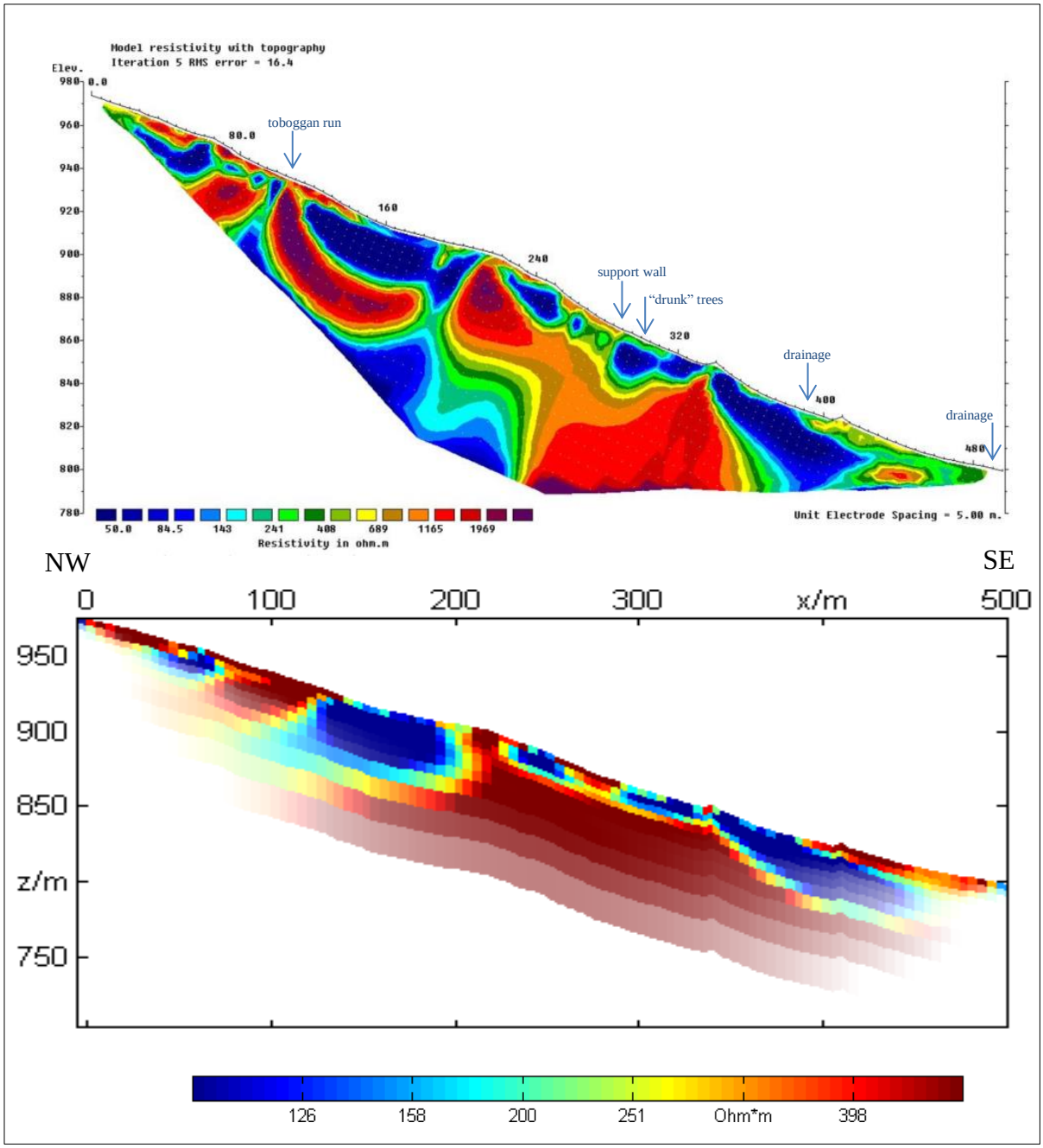


Figure 6-6 *DC2DInvRes* (lower) and *Res2dinv* (upper) tomography models for profile p3

6.1.4. ERT model p4

Profile p4 is shorter than other three profiles and is the only profile that is almost whole located in the mining quarry area.

According to Figures 6-1 and 6-2, as well as filed work notes, around 75 m there are two water conservation objects, and around 119 m and 145 m are open drainages. At 205 m is manhole, the same one as at the profile p1. At the beginning of profile, and from 80 m to 110 m, there are sub horizontal drainage pipes.

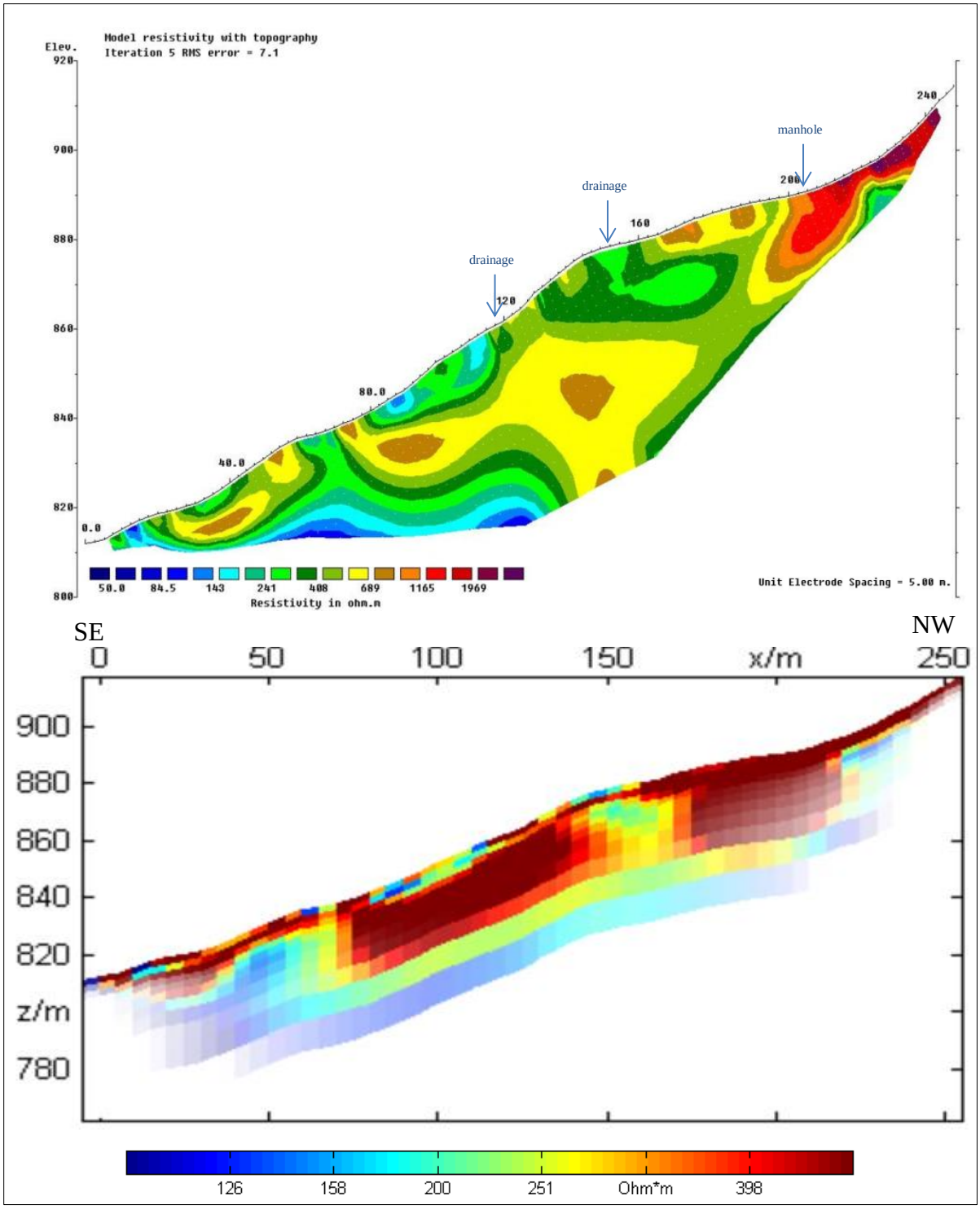


Figure 6-7 *DC2DInvRes* (lower) and *Res2dinv* (upper) tomography models for profile p4

After the first field work one profile needed to be chosen for monitoring. Several facts were considered before final decision. Finally, profile p4 was selected for monitoring purpose. One of the reasons was that profile p4 stretches through the part of quarry and it was important to monitor water exactly at the quarry area. Also, profile p4 is located

completely in the area of quarry and there are no problems with work there. For the purpose of monitoring, with the aim to observe changes in water presence, measurements in dry and wet period were needed to be performed.

Figure 6-8 shows the amount of rainfall at the periods of monitoring measurements, 24th May, 13th June and from 28th to 29th June.

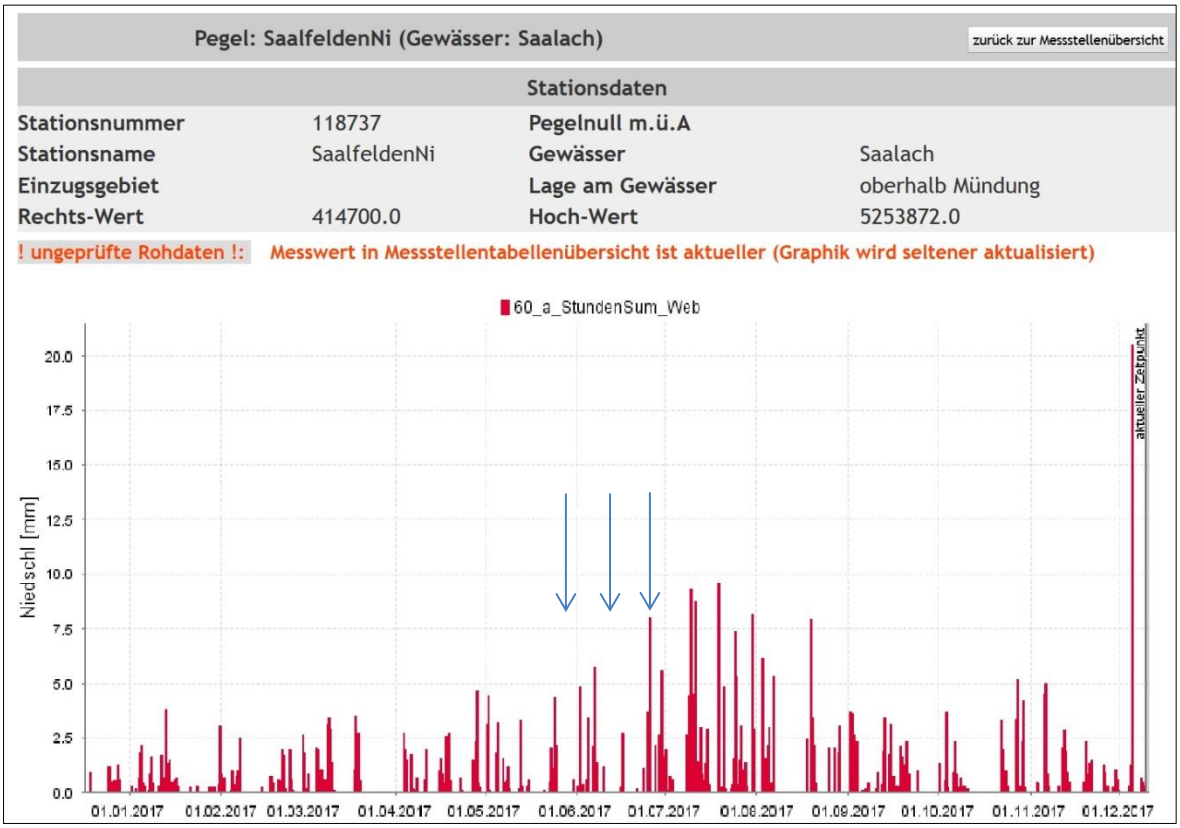


Figure 6-8 Rainfall [mm] with marked (blue arrow) periods of monitoring at profile p4 (https://www.salzburg.gv.at)

As shown, there were not any big rain events that could change the situation, what results also confirmed. The last monitoring measurement was done exactly during the big rain but it doesn't show any variation in results, as presented in Appendix 3.

Appendix 3 shows ten monitoring models in time lapse mode with the resistivity models during each measurement. The idea was to get insight if and how the underground condition is changing with more water supply. The first model shows the situation on May,

24th and the second on July, 13th. During both measurements there was insignificant precipitation. Next eight models are showing monitoring measurements from 28th to 29th July. Greater precipitation was expected as the forecast announced, but unfortunately only one big shower happened and the idea of monitoring couldn't show expected changes. Rain exactly started around the first measurement time and it didn't continue during the whole night. That way water didn't even have enough time to be infiltrated into subsurface (Appendix 3). Only barely visible changes are around 110 m where a broken drainage is located. Few hours after the first big shower, lower resistivity is visible in that part, but also after just few hours without water precipitation, area is again with the higher resistivity as previous.

Monitoring of the profile p4 didn't show any problem during average water precipitation, but it still keep an open question if the situation is the same with significant water precipitation.

6.2. Seismic-refraction models

The wide range of seismic velocities of rocks is partly because of lithology variations (Table 1). Important is that homogenous, consolidated, saturated, unweathered and intact rocks, have higher seismic velocities than heterogeneous, unconsolidated, unsaturated, weathered and fractured rocks (Everett, 2013). Rocks at greater burial depth are imposed to greater stress than shallower one so the degree of compactness decreases as well as density, what indicate higher seismic velocities (Šumanovac, 2007).

6.2.1. Seismic model P1

Seismic velocity model at profile P1 shows wide range of seismic velocities, from 600 m/s to 6000 m/s (Figure 6-9). Model is smooth, without details, so there cannot be seen compatibility with field work notes, such as locations of drainages. But seismic model P1 together with electric model p1 helped in defining geological profile GP-1.

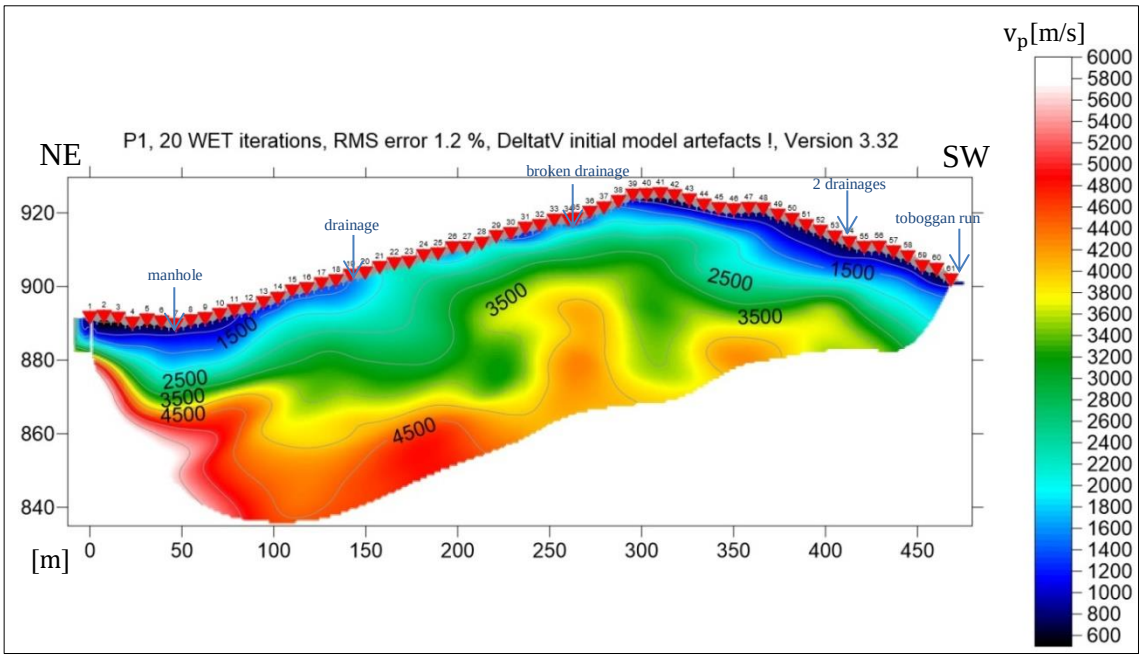


Figure 6-9 Seismic velocity model P1

6.2.2. Seismic model P4

At the seismic profile P4 the problem is insufficient number of shot points (Figure 6-11**)**. There were only three low energy hammer shots at locations of geophones 12, 35 and 46. Shot point spacing was too wide since shot spacing of 17 receivers between shot points

is much too wide for good quality of data interpretation. Figure 6-10 shows model of subsurface coverage of first break energy for profile P4. According to the processing of *Rayfract* software it would be necessary to record shots such that the shot spacing decreases to at least one shot per every 6th receiver position.

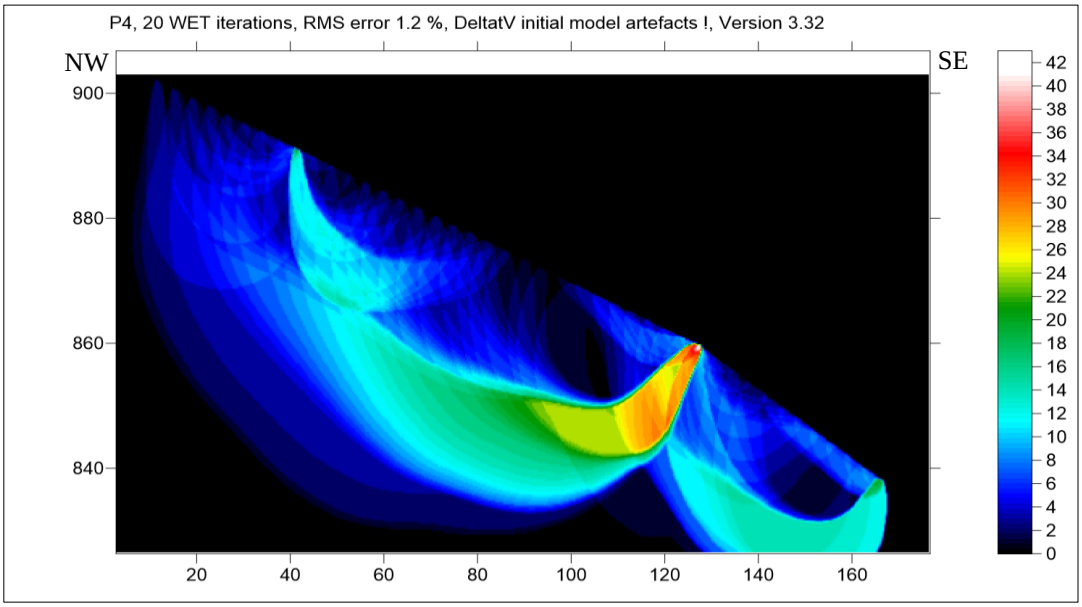


Figure 6-10 Coverage of subsurface with first break energy for profile P4

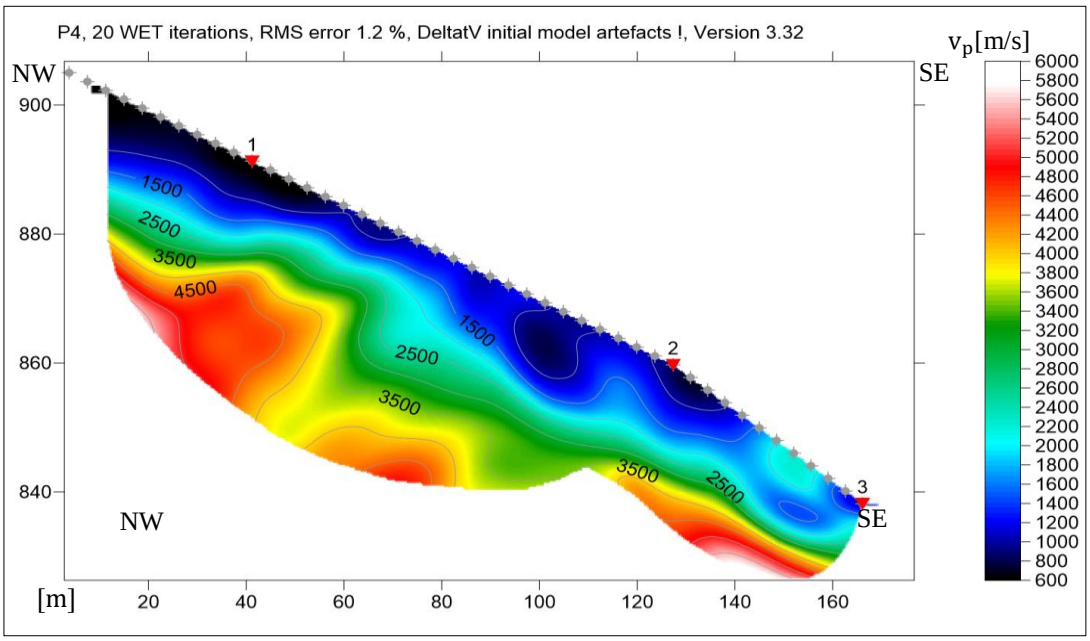


Figure 6-11 Seismic velocity model P4

7. Geological interpretation

Based on results of ERT and seismic refraction, as well as getting in correlation with previous investigations, positions of drainages and considering general geology of the area, two geological profiles were interpreted showing subsurface situation in the quarry area.

7.1. Geological profile GP-1

Figure 7-1 shows the geological interpretation according to ERT model p1 and seismic model P1. Basically, it contains four units, and these are clastic moraine materials, sediment rocks, metamorphic rocks and basement igneous rocks. Important role have the presented faults. At the geological profile GP-1 only two faults are included, but also sets of smaller faults are present.

At the beginning of the profile to the distance of 120 m, in the depth of around 30 m, geological unit of clastic moraine material, together with possible sandstones and greywacke deposits, is interpreted. They generally have lower seismic velocities, 600 – 2000 m/s, and higher resistivities, 500 – 1200 Ωm.

In the central part of the profile, from 120 m to 350 m, to the depth of 10 m, there are still greywacke rocks together with shales but mostly dominate metamorphic rocks like slate, quartzite and phyllite. Resistivities are still high, but seismic velocities are also greater, to 2500 m/s.

At the end of the profile, from 350 m to 480 m, and to the depth of 40 m, both resistivities (60 – 400 Ωm) and seismic velocities are low (700 – 2000 m/s). This can be explained by water presence in this area, since there are no drainage systems and rocks are saturated with water. Therefore, in this unit dominate saturated sand and clay as well as shale and slate.

The greatest geological unit is one of diabase. The diabase is igneous rock of basaltic composition that occurs mostly in shallow intrusions in form of dikes and sills. The fact that is a dike indicates its fragmentation that is favorable for water infiltration. Besides that, the faults are making it even more fractured and contribute to resistivity reduction. That explains this great diabase unit, in places highly fractured, characterized by wide

range of resistivities and seismic velocities. Resistivities are up to 3000 Ωm and seismic velocities up to 6000 m/s.

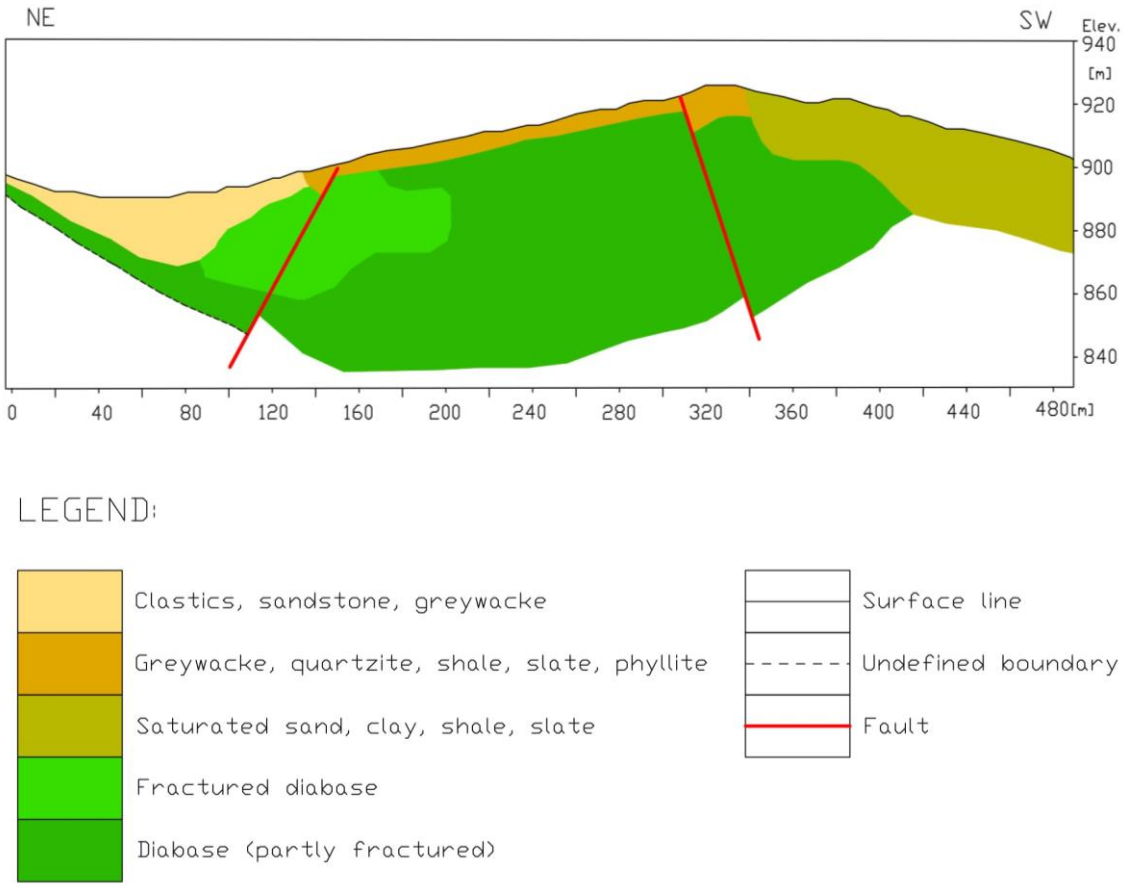


Figure 7-1 Geological profile GP-1

7.2. Geological profile GP-4

Figure 7-2 shows geological interpretation according to ERT model p4. Model of seismic velocities was not included in the interpretation because of low quality and unreliable results due to insufficiently number of shot points. The wave coverage was not sufficient to obtain reliable results.

Geological units, as expected, coincide with geological units at geological profile GP-1. Indeed great influence has the set of faults.

Until the distance of 180 m, with the depth range from 10 m to 30 m, are sediment rocks (greywacke, shale) and metamorphic rocks (quartzite, slate, phyllite).

In the last 60 m, with the depth range from 10 m to 40 m, are clastic moraine materials, sandstones and greywacke. The profile GP-4 at its distance of 205 m is crossing profile GP-1 at its 70 m, where geological units fit well.

The existence of the greatest geological unit, the diabase body, is explained the same as at the profile GP-1.

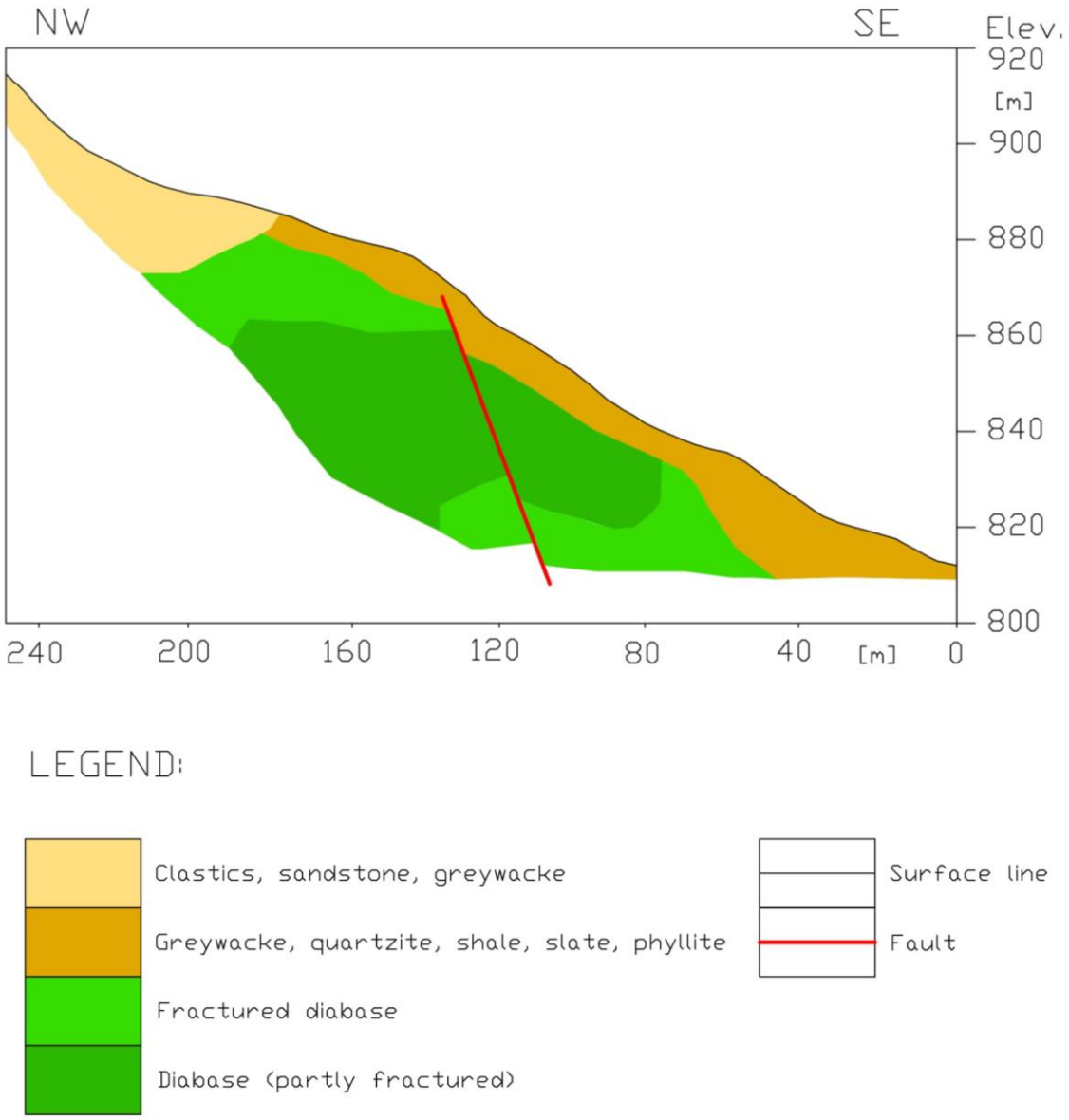


Figure 7-2 Geological profile GP-4

8. Conclusion

Geophysical research was performed to determine the lithological and structural relationships in the subsurface as well as presence of water and its influence. Therefore, electrical-resistivity method and seismic-refraction method have been applied. Four electrical profiles (p1, p2, p3, p4) and two seismic profiles (P1 and P4) were measured. The electrical-resistivity tomography models obtained by *DC2DInvRes* and *Res2dinv* software coincide well. Seismic model P1 largely coincides with an electrical model p1, while seismic model P4 is unreliable because of low quality recorded data due to insufficiently number of the shot positions. Afterwards, electrical model p1 together with seismic model P1, were used to construct geological profile GP-1. Also, electrical model p4 helped in interpretation of geological profile GP-4.

The first and the second electrical models, p1 and p2, generally indicated the presence of big diabase body, more or less fractured. The diabase has the greatest resistivities, but they are in the range from 400 Ωm to 3000 Ωm, probably because of its dike nature. Prominent faulting causes fracturing of rocks and contributes to the resistivity reduction. Those locations are well covered by drainage system, which is shown at resistivity models by higher resistivities. The ends of profiles are not drained and lower resistivities are present there, as well as lower seismic velocities that are obtained at seismic model P1. That refers to saturated rocks and it must be considered to protect this area with water drainage.

The third ERT model p3 is showing two wide areas of moraine material. Resistivities are considerably low, around 50 Ωm, and more attention should be paid to draining this area. It is important to protect it because it is parallel with summer touristic attraction, toboggan run. Supporting walls would be one of possible aid to prevent probable land sliding.

The forth ERT model p4 that is located mostly in quarry area was also interpreted as big diabase unit, also faulted, and significant metamorphic rocks. This area is well drained and monitoring didn’t show any features that would be challenging. But it would be recommended to repeat monitoring measurement before and after great rainfall event.

It is known that extreme access of water and high water pressures have a destabilizing effect on slopes. The general drainage of surface water from quarry mining area is very efficient method to stabilize possible slopes. For constructing support and safety structures, it is important to ensure that no water pressure builds up behind the supporting structure. Proven good management and previous experience gained in quarry at Saalfelden, shows that even in the case of very difficult geotechnical and hydrogeological conditions it is possible to manage a safe opencast mine and installation of additional drainage system as well as building supporting walls that could be helpful in further operating a safe mining.

9. Bibliography

ANTHES, G., HEUGENHAUSER, R., MAYR, C., WAGNER, H. (2011). Der Hinterburgbruch in Saalfelden: Stabilisierung von Felsbewegungen in einem wassereichen Tagebau. Berg- und Huettenmannische Monatshefte, Austria.

EVERETT, M.E. (2013). Near-Surface Applied Geophysics. Texas A&M University, Cambridge University Press.

GEBRANDE, H., MILLER, H. (1985). Refraktionsseismik, in Angewandte Geowissenschaften II, Methoden der Angewandten Geophysik und mathematische Verfahren in Geowissenschaften, edited by F. Bender, pp. 226-260 F. Enke Verlag, Stuttgart.

GOLDBRUNNER, J.E. (2000). Hydrogeology of Deep Groundwaters in Austria. Mitt. Osterr. Gool. Ges., ISSN 0251-7493, pp. 281-294, Vienna.

GRIFFITHS, D.H., BARKER, R.D. (1993). Two-dimensional resistivity imaging and modelling in areas of complex geology. Journal of Applied Geophysics, 29, 211-226.

LOKE, M.H. (2000). Electrical Imaging Surveys for Environmental and Engineering Studies: A Practical Guide to 2-D and 3-D Surveys. Available at: www.geometrics.com.

Rayfract (2006). Manual of *Rayfract* software, version 3.32, Intelligent Resources Inc. (1996-2006).

RAUEN, A. (2016). Manual of *GeoTest* software, version 2.46.

ŠUMANOVAC, F., (2007). Geofizička istraživanja podzemnih voda. Rudarsko-geološko-naftni fakultet, Sveučilište u Zagrebu, Pauk Cerna.

ŠUMANOVAC, F., (2012). Osnove geofizičkih istraživanja. Rudarsko-geološko-naftni fakultet, Sveučilište u Zagrebu.

WINKLER, G., HILBERG, S. (2016). Hydrogeology of Austria: Selected Papers. Austrian Journal of Earth Sciences, Volume 109/1, Vienna.

Internet sources:

http://www.geoland.at/geo_webgis/(S(gdheszba1yqfkyqwajpx13ss))/init.aspx (13.12.2017.)

http://www.arcgis.com/home/webmap/viewer.html?webmap=c1255d236ac84cd68fc02fd037a5ed8d&extent=9.5714,46.0148,17.1246,49.3562 (05.06.2017.)

https://weather-and-climate.com/average-monthly-Rainfall-Temperature-Sunshine,Salzburg,Austria (14.12.2017.)

https://www.salzburg.gv.at/wasserwirtschaft/6-64-seen/hdweb/stations/118737/station.html (28.12.2017.)

APPENDICES

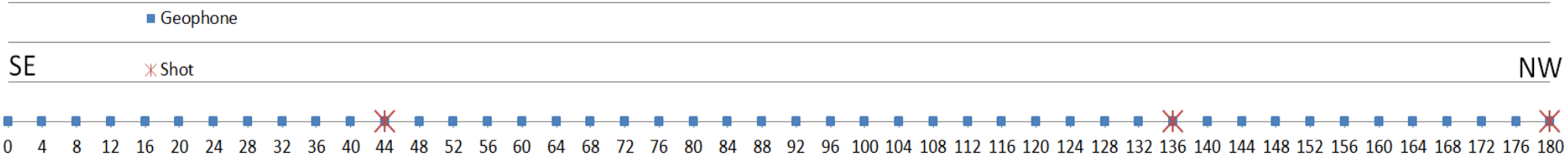
Appendix 1 Spreadsheet of recording geometry for seismic model P1

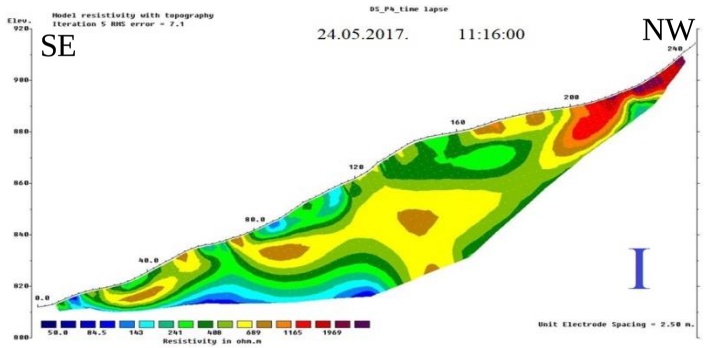
REC.	GEOPHONE	PROFILE (m)	ALTITUDE (m)	EAST (m)	NORTH (m)
1	1	0	891.55	334938.91	5255104.59
2	3	8	891.81	334938.91	5255096.91
3	5	16	891.33	334938.91	5255089.23
4	7	24	890.00	334938.45	5255081.43
5	9	32	890.87	334937.58	5255073.60
6	11	40	890.32	334936.66	5255065.76
7	13	48	889.63	334933.13	5255058.65
8	15	56	890.65	334929.59	5255051.58
9	17	64	891.22	334926.70	5255044.24
10	19	72	892.35	334924.38	5255036.67
11	21	80	893.40	334922.06	5255029.11
12	23	88	893.78	334917.99	5255022.34
13	25	96	895.58	334913.89	5255015.57
14	27	104	896.73	334909.20	5255009.28
15	29	112	898.69	334903.98	5255003.44
16	31	120	899.34	334898.75	5254997.52
17	33	128	900.74	334893.00	5254992.01
18	35	136	901.52	334887.24	5254986.50
19	37	144	902.98	334882.14	5254980.50
20	39	152	903.61	334877.60	5254974.01
21	41	160	905.09	334873.07	5254967.52
22	43	168	906.16	334868.95	5254960.66
23	45	176	906.51	334864.78	5254953.80
24	47	184	908.30	334860.62	5254947.06
25	49	192	908.81	334856.50	5254940.41
26	51	200	910.45	334852.33	5254933.75
27	53	208	910.50	334848.05	5254927.06
28	55	216	911.66	334843.72	5254920.40
29	57	224	913.51	334839.38	5254913.78
30	59	232	914.32	334835.07	5254907.21
31	61	240	915.77	334830.71	5254900.58
32	63	248	916.51	334825.90	5254894.37
33	65	256	917.96	334821.10	5254888.15
34	67	264	917.95	334816.29	5254882.03
35	68	268	918.31	334813.84	5254879.03
36	70	276	920.09	334808.98	5254873.05
37	72	284	921.29	334805.13	5254866.42
38	74	292	923.01	334802.27	5254859.12
39	76	300	924.79	334799.37	5254851.82
40	78	308	924.91	334799.00	5254844.33

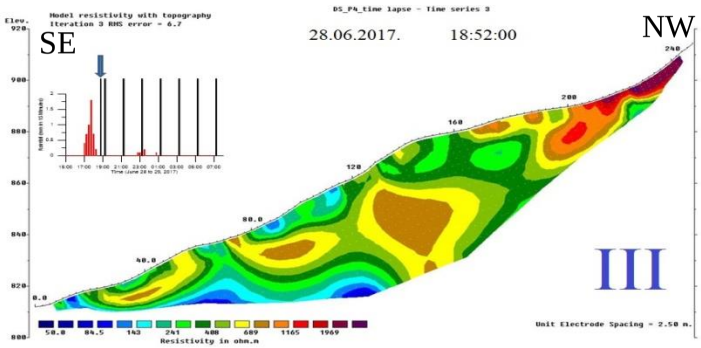
41	80	316	925.14	334798.60	5254836.80
42	82	324	924.65	334798.91	5254829.09
43	84	332	923.46	334799.91	5254821.15
44	86	340	922.07	334800.95	5254813.26
45	88	348	921.08	334802.31	5254805.23
46	90	356	920.80	334803.68	5254797.25
47	92	364	921.15	334805.26	5254789.35
48	94	372	921.03	334807.08	5254781.55
49	96	380	919.32	334808.89	5254773.79
50	98	388	918.15	334809.48	5254766.13
51	100	396	916.49	334810.07	5254758.46
52	102	404	914.94	334809.75	5254750.75
53	104	412	913.39	334808.53	5254742.99
54	106	420	911.86	334807.26	5254735.23
55	108	428	910.55	334804.95	5254727.52
56	110	436	910.61	334802.63	5254719.81
57	112	444	909.35	334800.57	5254712.15
58	114	452.7	908.02	334798.68	5254704.57
59	116	460	905.38	334796.83	5254696.96
60	118	468	904.61	334795.44	5254689.30
61	120	476	901.75	334794.09	5254681.68

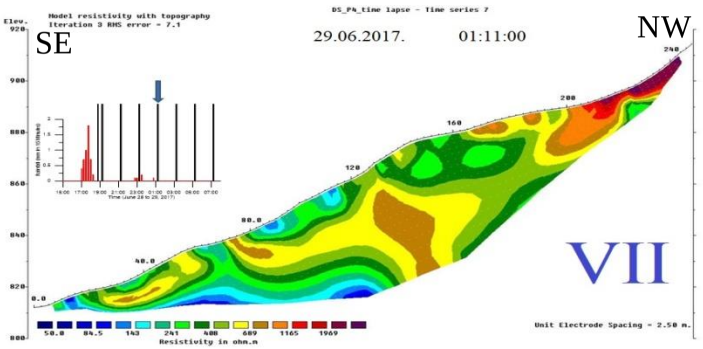
Appendix 2 Spreadsheet (up) and graphic display (down) of recording geometry for seismic model P4

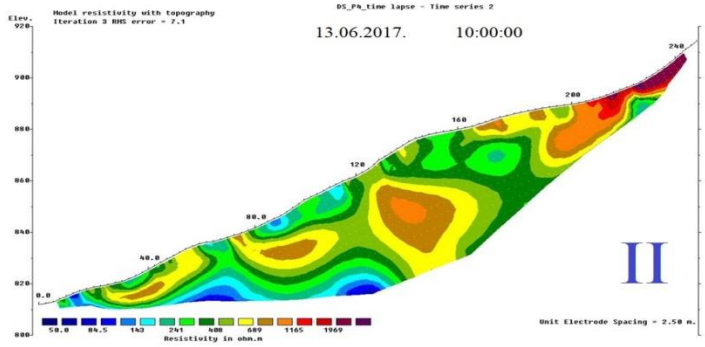
REC.	1	2	3
GEOPHONE	12	35	46
PROFILE (m)	44	136	180
ALTITUDE (m)	891.28	859.71	838.18
EAST (m)	334930.90	334993.98	335017.42
NORTH (m)	5255059.00	5255000.31	5254969.45

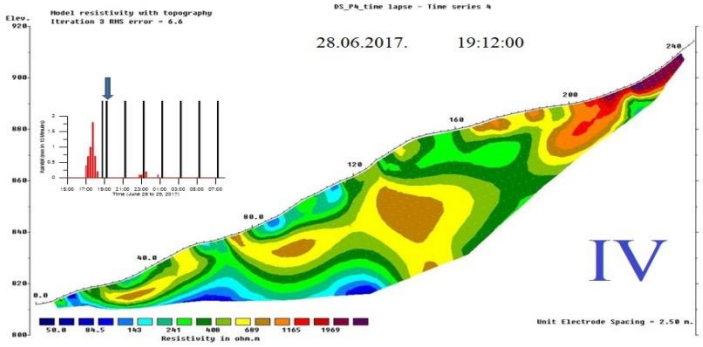


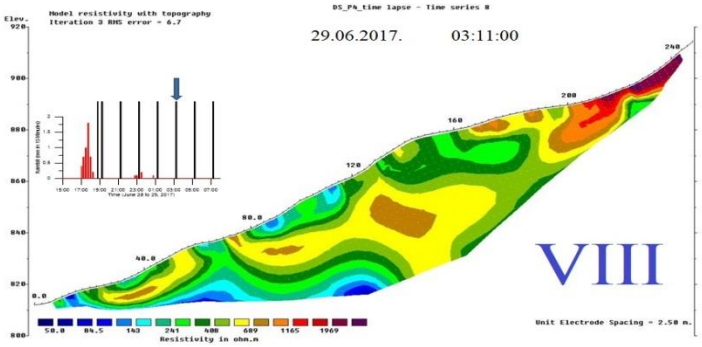


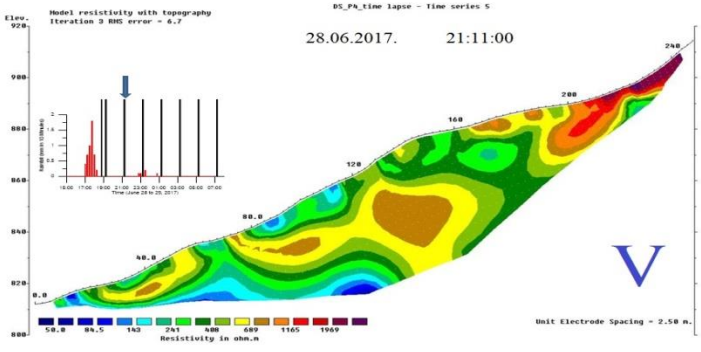


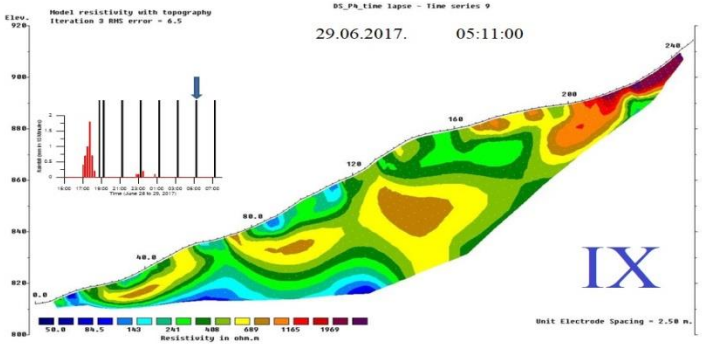


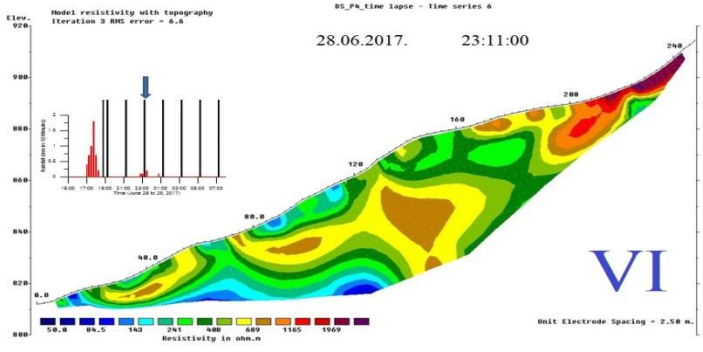


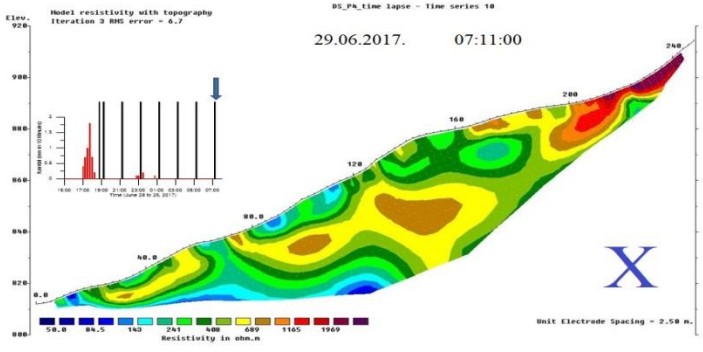












Appendix 3 ERT monitoring models for profile p4